

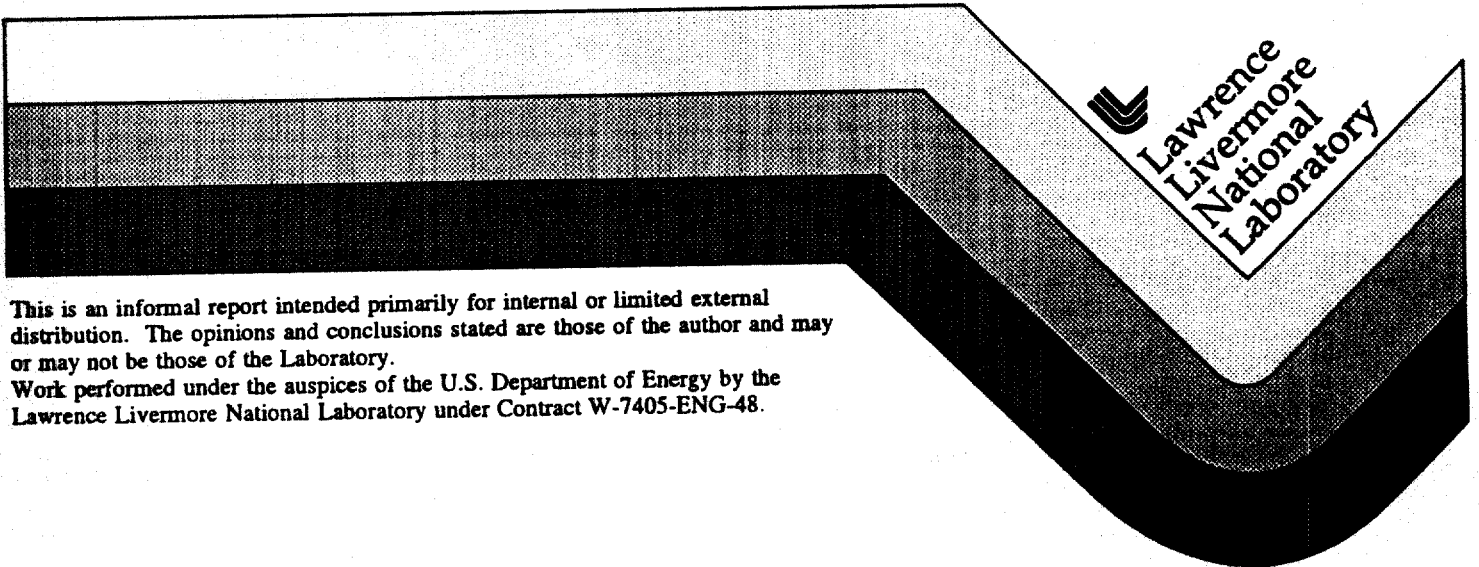
2 31791

UCRL-ID-125017

KESTI Containment Data Report

T. Stubbs
R. Heinle

March 1996



This is an informal report intended primarily for internal or limited external distribution. The opinions and conclusions stated are those of the author and may or may not be those of the Laboratory.

Work performed under the auspices of the U.S. Department of Energy by the Lawrence Livermore National Laboratory under Contract W-7405-ENG-48.

DISCLAIMER

This document was prepared as an account of work sponsored by an agency of the United States Government. Neither the United States Government nor the University of California nor any of their employees, makes any warranty, express or implied, or assumes any legal liability or responsibility for the accuracy, completeness, or usefulness of any information, apparatus, product, or process disclosed, or represents that its use would not infringe privately owned rights. Reference herein to any specific commercial products, process, or service by trade name, trademark, manufacturer, or otherwise, does not necessarily constitute or imply its endorsement, recommendation, or favoring by the United States Government or the University of California. The views and opinions of authors expressed herein do not necessarily state or reflect those of the United States Government or the University of California, and shall not be used for advertising or product endorsement purposes.

This report has been reproduced
directly from the best available copy.

Available to DOE and DOE contractors from the
Office of Scientific and Technical Information
P.O. Box 62, Oak Ridge, TN 37831
Prices available from (615) 576-8401, FTS 626-8401

Available to the public from the
National Technical Information Service
U.S. Department of Commerce
5285 Port Royal Road
Springfield, VA 22161

KESTI Instrumentation Summary

Instrumentation	Fielded on this Event	Data Return	Present in this Report
<u>Plug Emplacement</u>	yes	yes	yes
<u>Radiation</u>	yes	yes	yes
<u>Pressure</u>			
Stemming	yes	yes	yes
Challenge	no	-	-
Cavity	no	-	-
Atmospheric	no	-	-
<u>Motion</u>			
Free Field	no	-	-
Surface	yes	yes	yes
Plug	yes	yes	yes
Stemming	no	-	-
Surface Casing	no	-	-
Emplacement Pipe	no	-	-
<u>Hydroyield</u> (a)	yes	yes	no
<u>Collapse</u> (b)	yes	yes	yes
<u>Stress</u>	no	-	-
<u>Strain</u> (c)	yes	yes	no
<u>Other Measurements</u> (d)	yes	yes	yes

- (a) CORTEX and/or SLIFER in emplacement hole.
- (b) EXCOR or CLIPER in emplacement hole.
- (c) Strain load on emplacement pipe.
- (d) Pressure and temperature in the device canister.

Event Personnel

Containment Physics

B. Hudson	LLNL
W. Woodward	LLNL
J. Kalinowski	EG&G/AVO
T. Stubbs	EG&G/AVO

Instrumentation

C. Cordill	LLNL
M. Hatch	EG&G/AVO
W. Webb	EG&G/NVO
L. Farthing	EG&G/NVO

1. Event Description

1.1 Site

The KESTI event was detonated in hole U9cn of the Nevada Test Site as indicated in figure 1.1. The KESTI device had a depth-of-burial (DOB) of 289 m in the Tunnel bed Tufts of area 9, about 135 m above the Paleozoic formation and 290 m above the standing water level, as shown in figure 1.2⁽¹⁾. Figure 1.3 is a plan map of the immediate vicinity of hole U9cn showing the drill holes used in the construction of the cross section plot of figure 1.2. Stemming of the 2.44 m diameter emplacement hole followed the plan shown in figure 1.4. A log of the stemming operations was maintained by Holmes & Narver⁽²⁾.

Detonation time was 12:20 PST on March 26, 1983, and collapse progressed to the surface at about 1 hour after detonation. Surface expression of the collapse was a slight depression at surface ground zero (SGZ) with some radial and circumferential surface cracks evident to a distance on the order of a hundred metres from ground zero.

No radiation arrivals were detected above ground and the KESTI containment was considered successful.

1.2 Instrumentation

Figure 1.5 is a schematic layout of the instrumentation designed to monitor the emplacement procedures and stemming performance of the KESTI event.

Three of the four stemming plugs above the KESTI event were composed of rigid coal-tar epoxy (LAE 59, denoted CTE) about 3 m thick. A soft, 1.5 m thick, layer of coal-tar and aggregate (LAE 59MY, denoted CTA) was poured on the top of the second and fourth (top) plugs to act as a gas seal while plug 1 (the deepest) was a 3.3 m thick layer of CTA over a layer of fines material.

Pressure and radiation were monitored at six places in the coarse stemming material, as shown in figure 1.5. To assess the efficacy of the deep, soft stemming plug as a gas block, pressure and radiation stations were fielded on either side of this structure. Two stations were mounted in the long stemming section between the deep soft plug and the first rigid plug (plug 2) with an additional station below each of the two upper plugs.

Gas pressure and temperature measurements were attempted in a line-of-sight pipe within the device canister. These quantities were monitored on either side of a baffle within the pipe. Strain (load) on the emplacement pipe was monitored during emplacement and noted from time to time in the stemming log⁽²⁾.

Vertical motion of the stemming plugs as well as the motion of the ground surface, 15.42 m from SGZ was monitored.

Data from each of the above instruments were transmitted to the recording trailer by an analog system and recorded on magnetic tape.

D-cable information was used for quality assurance during the stemming operations. Two CLIPER sensors were mounted in the emplacement hole to monitor cavity collapse and chimney formation; one attached to the device canister and emplacement pipe and one in the emplacement hole with the containment gauge pendant.

A history of the fielding operations of the instrumentation is outlined in reference 4. Details of the instrumentation are given in reference 5.

1.3. Emplacement

The stemming plugs consisted of three "LAE 59" coal-tar epoxy (CTE) layers and a bottom plug of soft, coal-tar-aggregate "LAE 59MY" (CTA). The bottom plug was about 3.3 m thick while the CTE plugs were about 3 m thick. Plugs 2 and 4 were capped with about 1.5 m of CTA to act as a gas sealant. Stemming between the plugs consisted of layers of fines and coarse gravel. The top of the hole (above the top plug) was filled with ground surface derived backfill and the inside of the emplacement pipe was grouted for its full length. See figure 1.4.

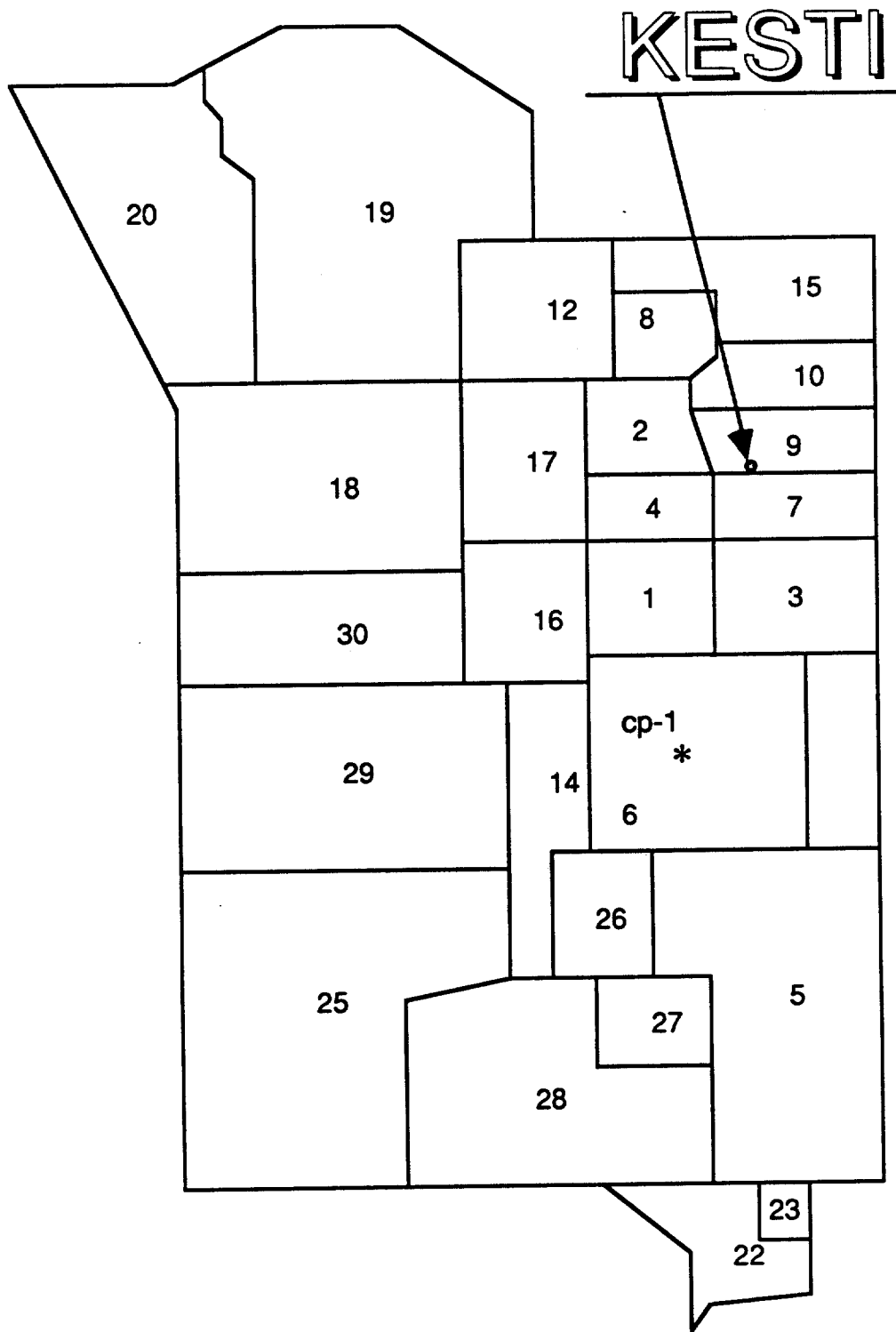


Figure 1.1 Map of the Nevada Test Site indicating the location of hole U9cn.

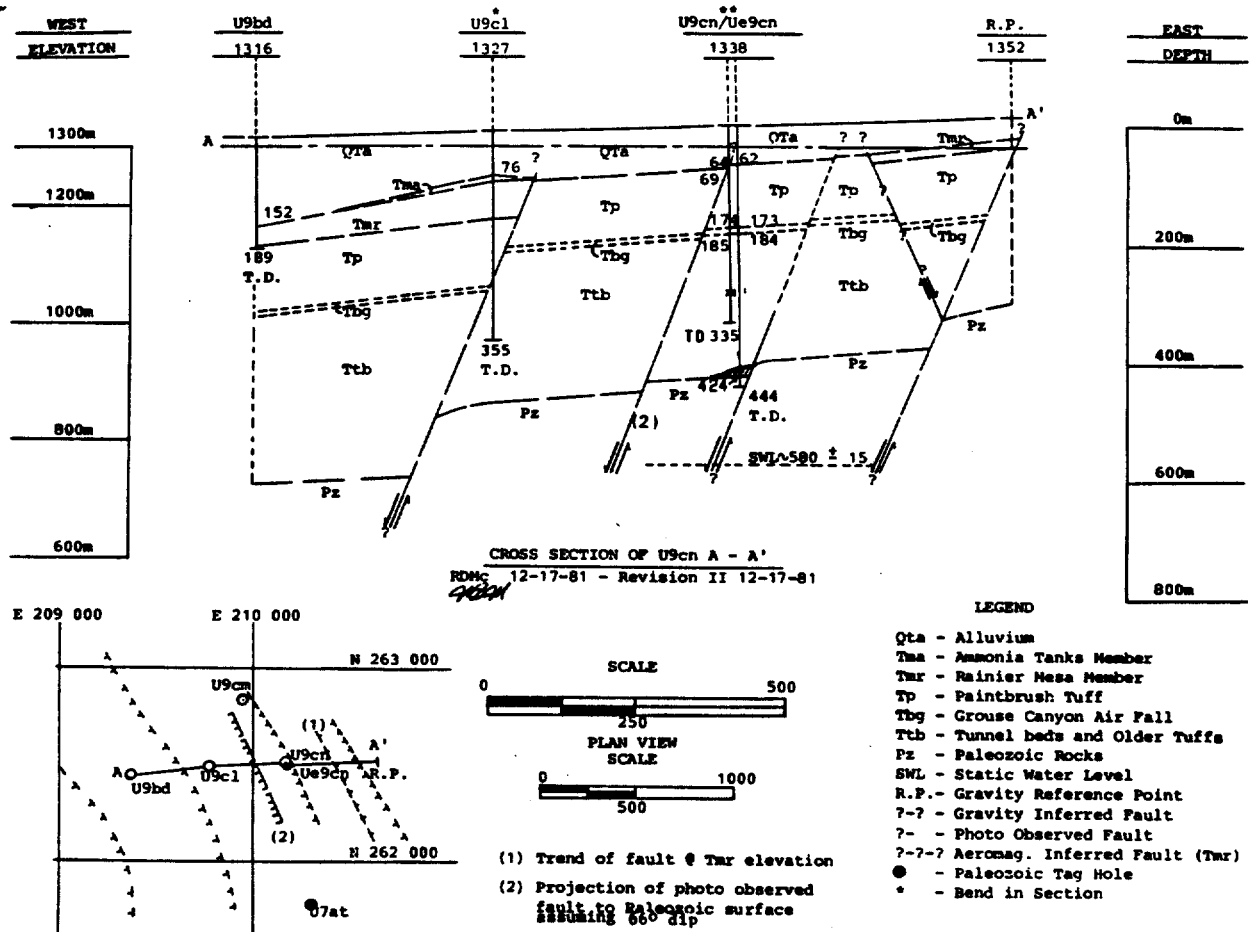


Figure 1.2 East-West geologic cross section through hole U9cn.

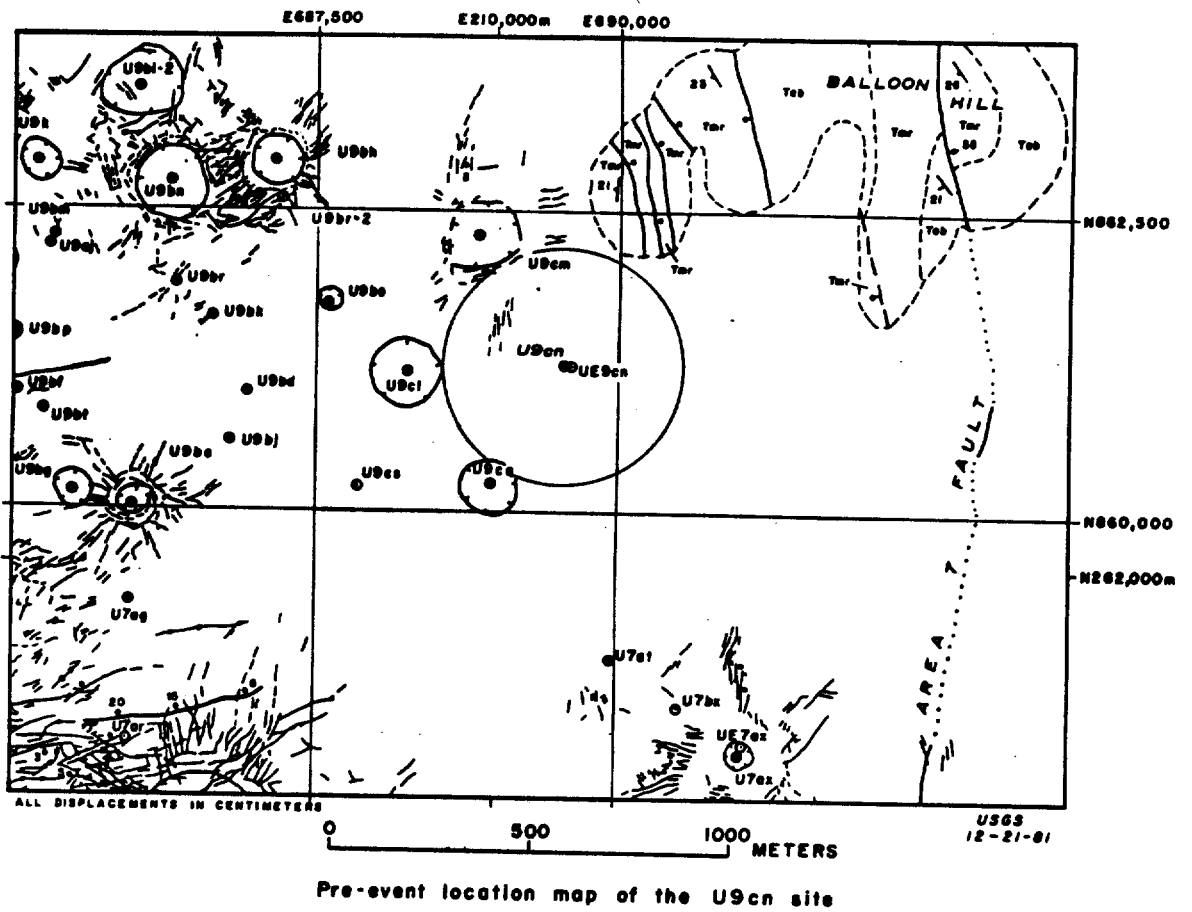
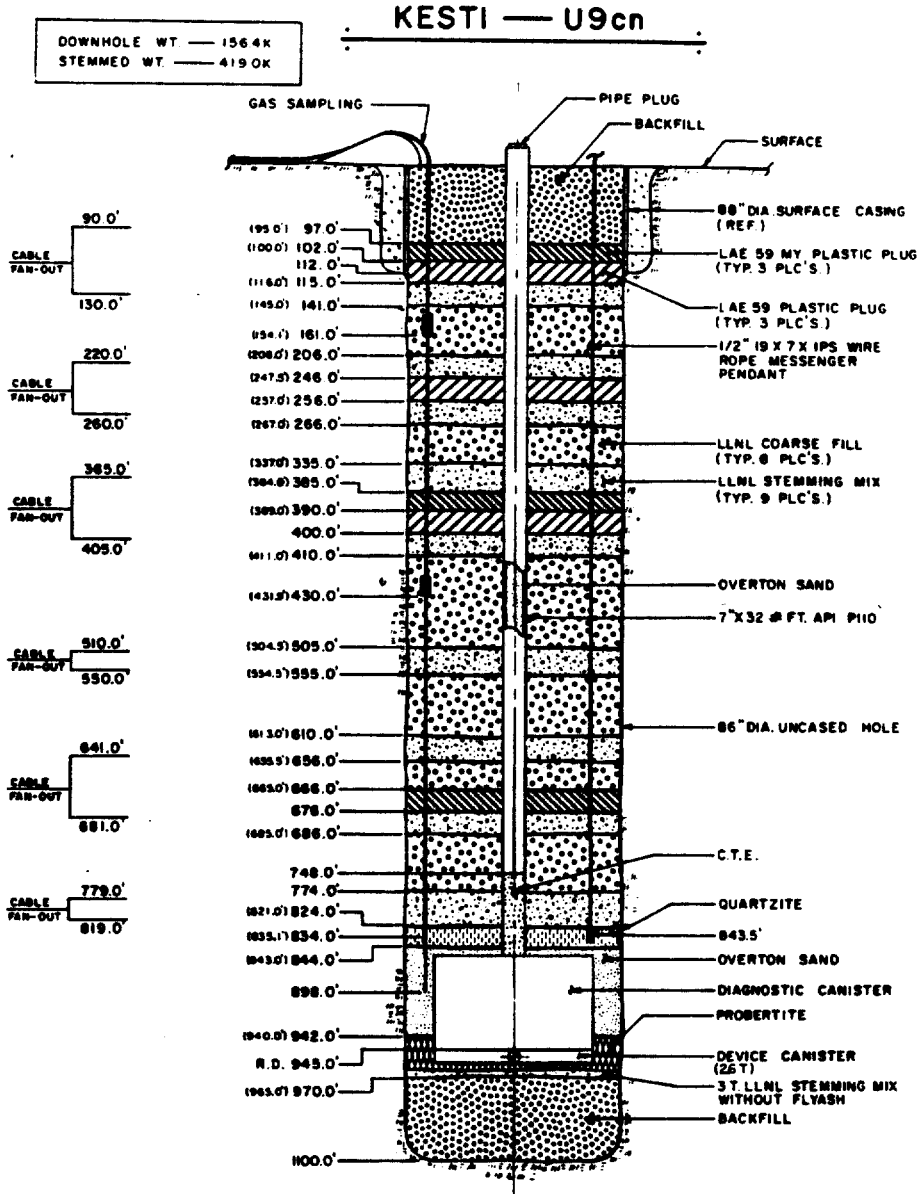


Figure 1.3 Plan View Map of the region encompassing hole U9cn showing the holes used in the geologic cross section of figure 1.2.



LEGEND: (XXX) DENOTES ACTUAL

HOLMES & HARVER INC.

Figure 1.4 As-built stemming plan for the event KESTI in Hole U9cn.

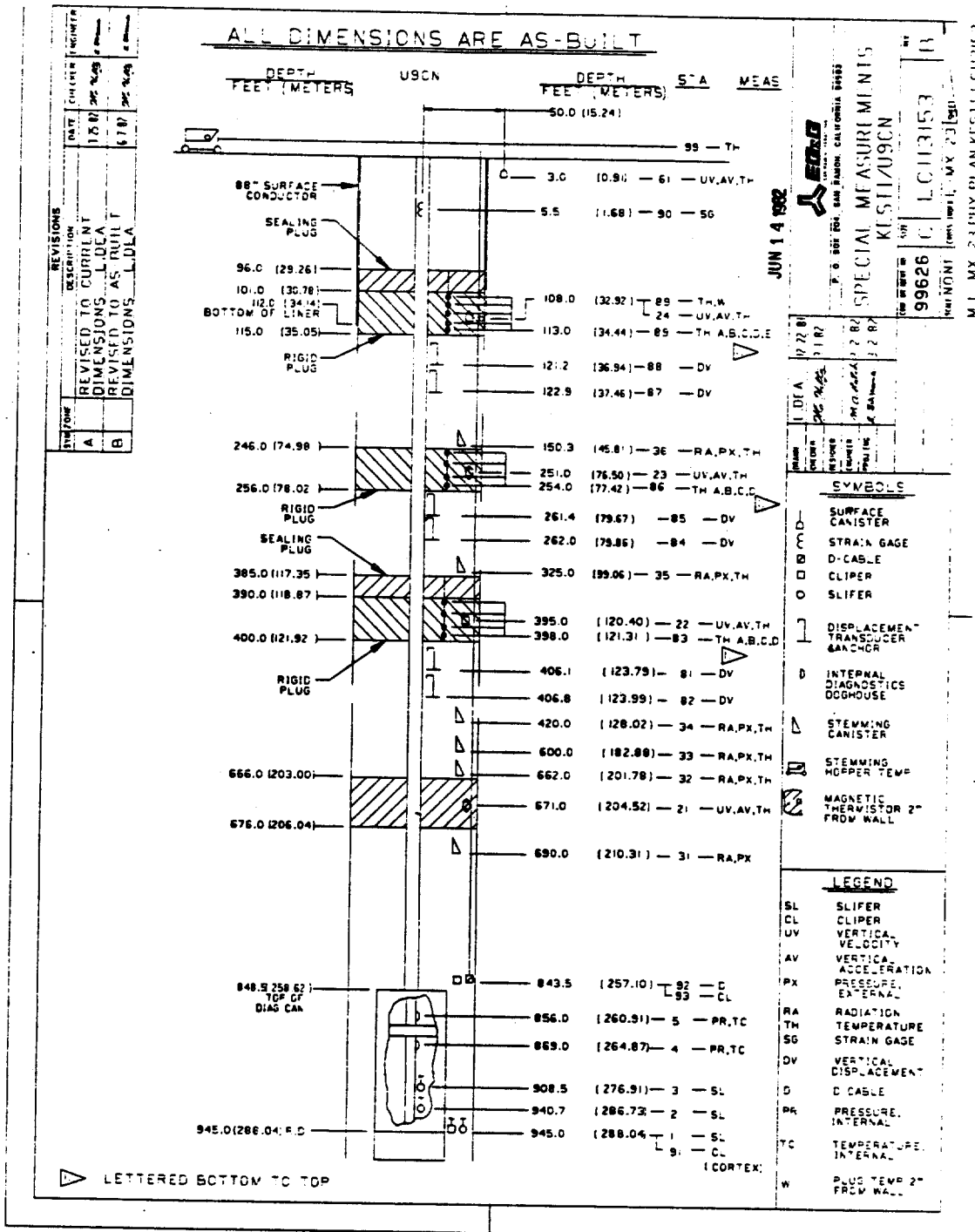


Figure 1.5 As-built containment instrumentation plan for the emplacement hole (U9cn) on the KESTI event.

2. Stemming Performance

2.1 Radiation and Pressure

Pressure and radiation were monitored on the KESTI event at six stations in the coarse stemming of the emplacement hole and the wave forms of these measurements are shown in figures 2.1–2.6. Figure 2.7 is a composite plot of all of the radiation wave forms with each corresponding base line (0.001 R/Hr) at the vertical position of its station. A brief report⁽⁶⁾ was issued previously.

Two radiation arrivals are seen in the data from station 31 (figure 2.1) at 155 s and about 1100 s. This later arrival is absent from all stations at higher elevation. In figure 2.7 the first arrival is seen to progress monotonically up the hole with an arrival time at station 36 of about 500 s and with the wave form at all stations above 31 being similar. It is postulated that this first arrival is "shine" from the prompt gas sampling hose which was mounted within 0.7 m of all of the radiation stations.

Early time pressure changes are consistent with ground motion and no pressure change is observable at the time of the second radiation arrival at station 31 (figure 2.1). This indicates that the bottom plug was not severely challenged by the cavity gases.

The radiation data are consistent with satisfactory containment.

2.2 Motion

Explosion-induced histories of the motion measured on the KESTI event are shown in figures 2.8–2.12. Characteristics of the associated motion and transducers are given in tables 2.1–2.3.

2.3 Collapse phenomena

Motion measured during collapse is shown in figures 2.13–2.17. Figure 2.18 shows the output of CLIPER station 93 (mounted with the containment instrumentation pendant) along with the displacement histories derived from the velocity transducers mounted in the stemming plugs. The ground surface near SGZ (figures 2.16 and 2.17 shows less than -1 m permanent displacement, agreeing with the "slight depression of the surface" noted earlier. The CLIPER mounted on the device canister and emplacement pipe (station 91) did not yield useful information.

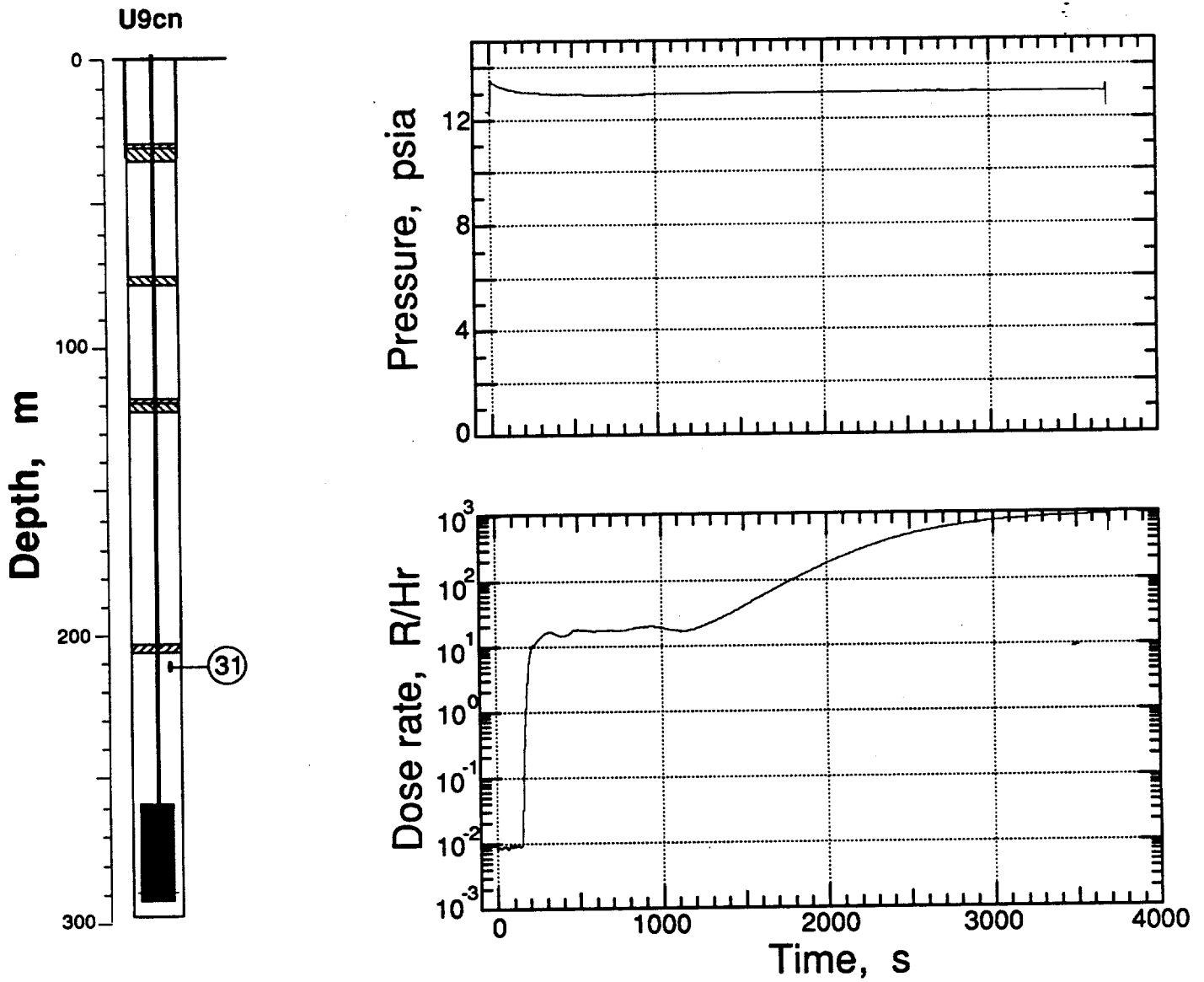


Figure 2.1 Pressure and radiation measured in the coarse stemming below the bottom plug (station 31 at a depth of 210.3 m).

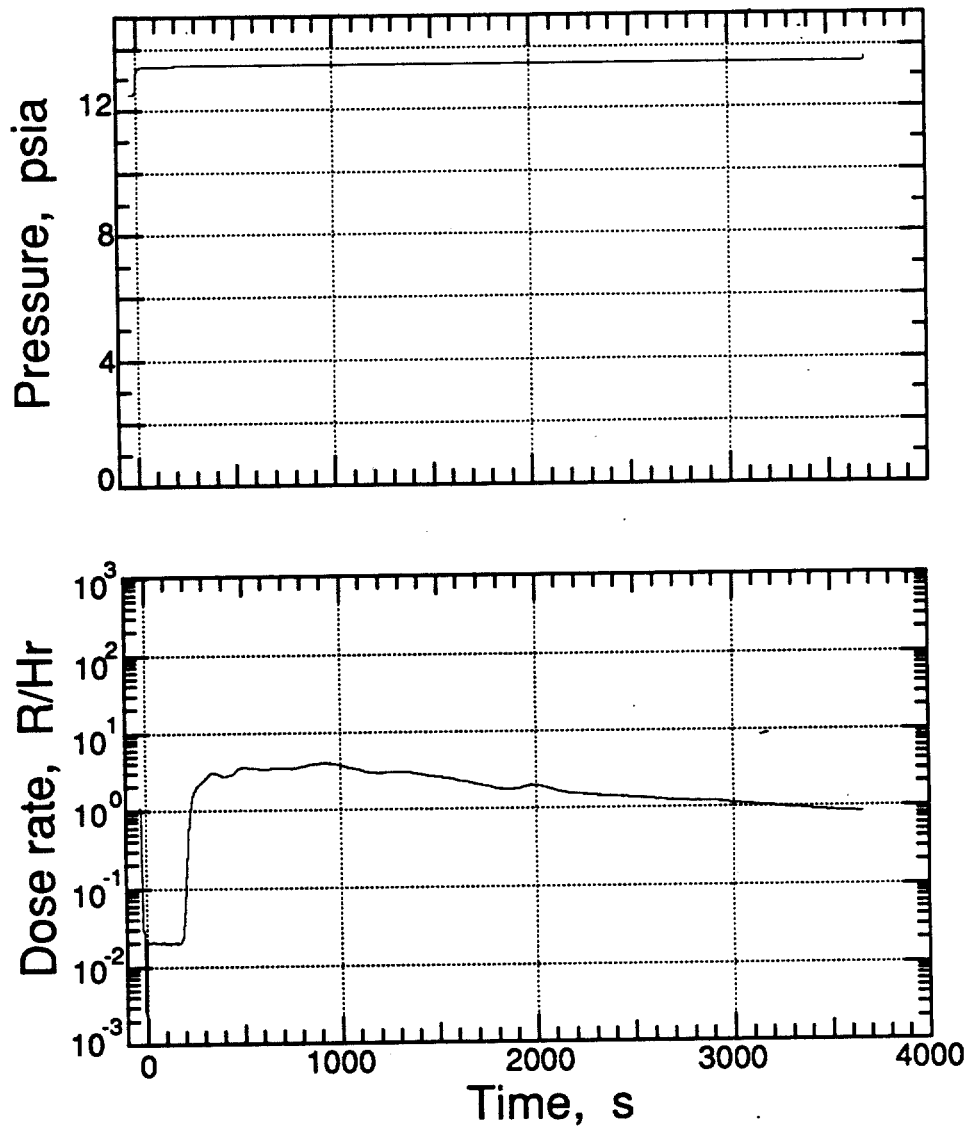
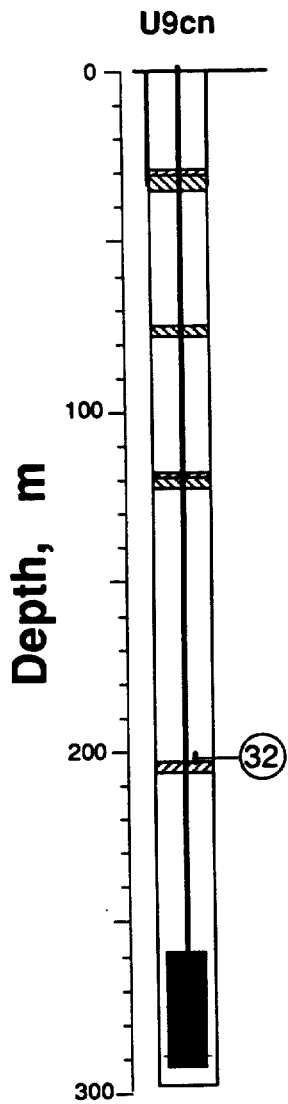


Figure 2.2 Pressure and radiation measured in the coarse stemming above the bottom plug (station 32 at a depth of 201.8 m).

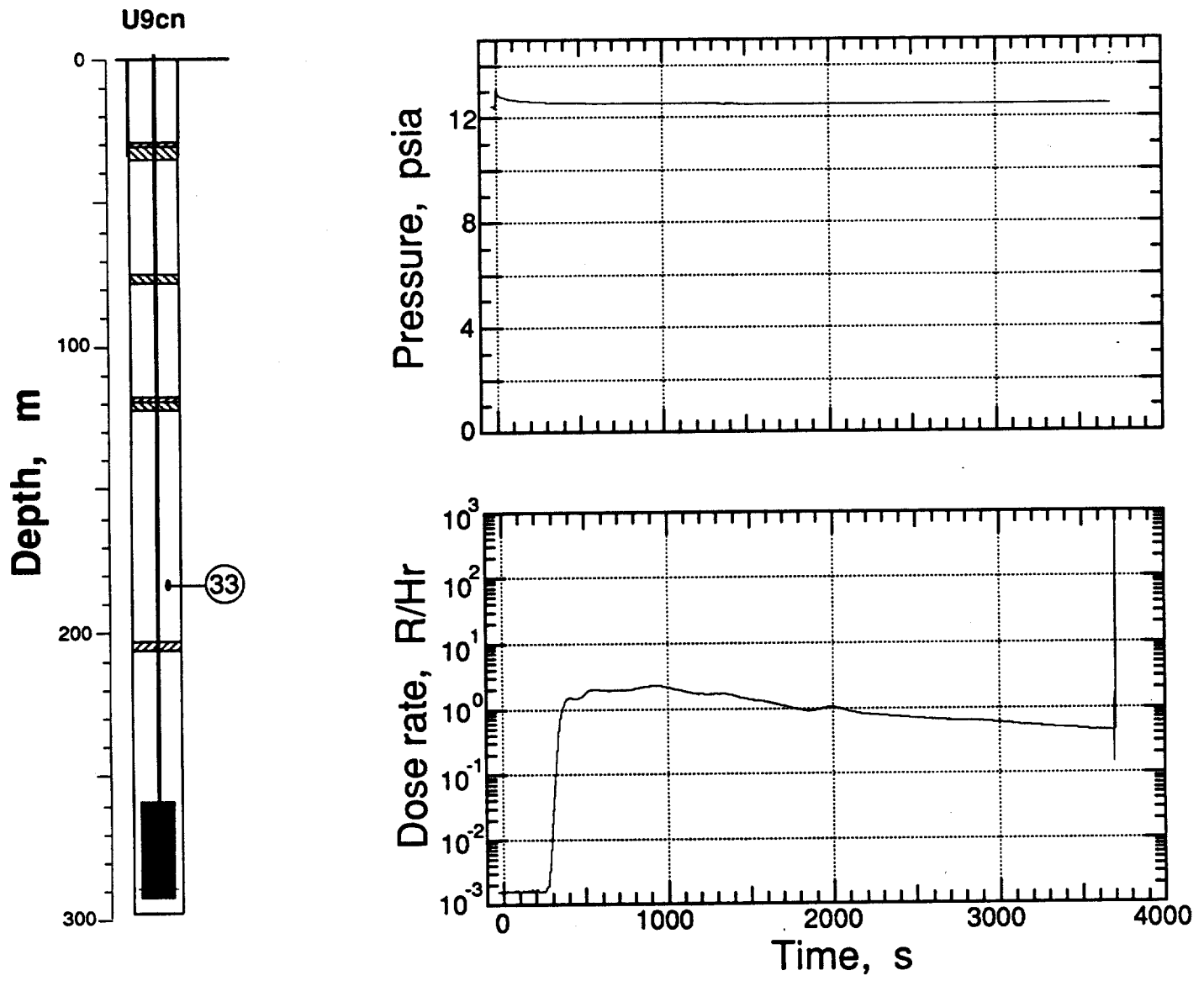


Figure 2.3 Pressure and radiation measured in the coarse stemming between plugs 1 and 2 (station 33 at a depth of 182.9 m).

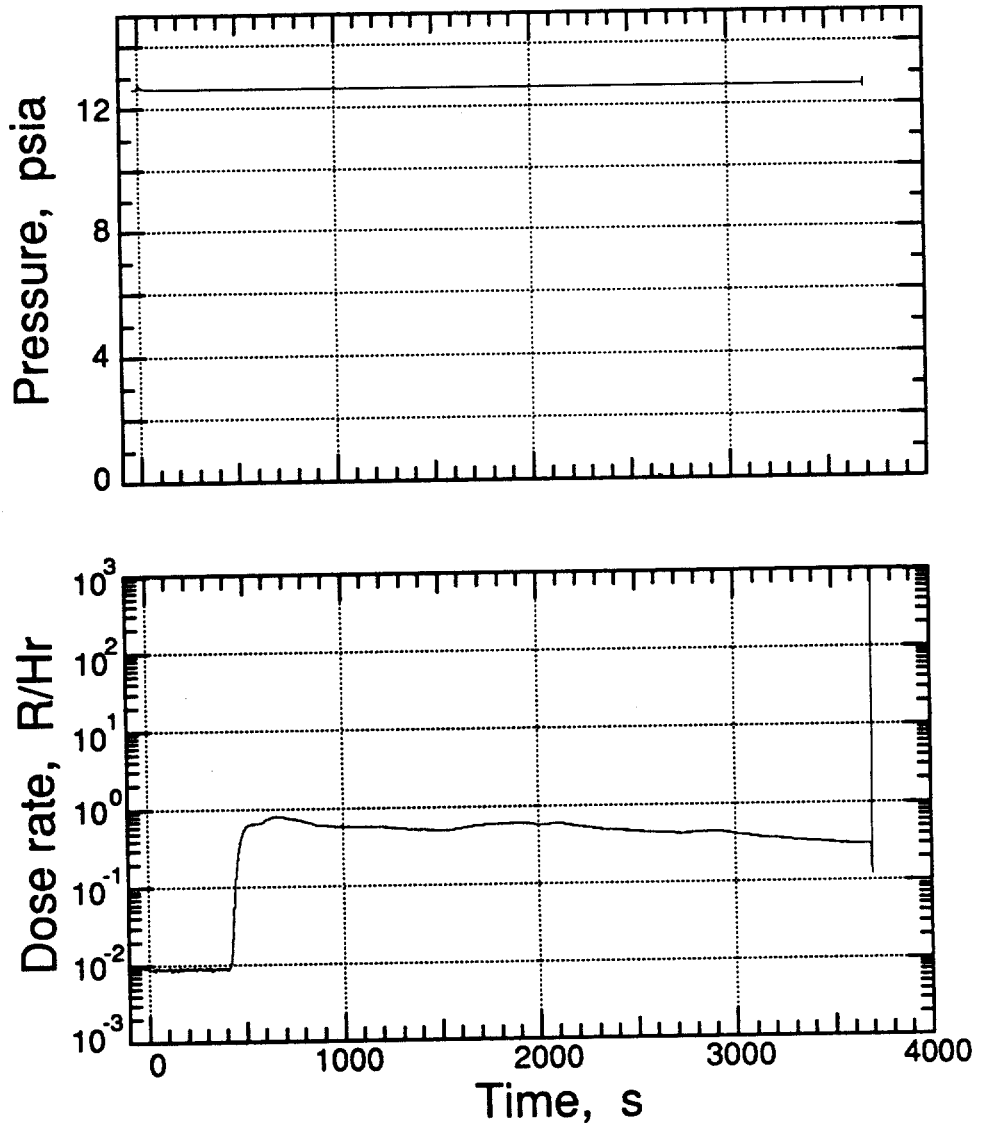
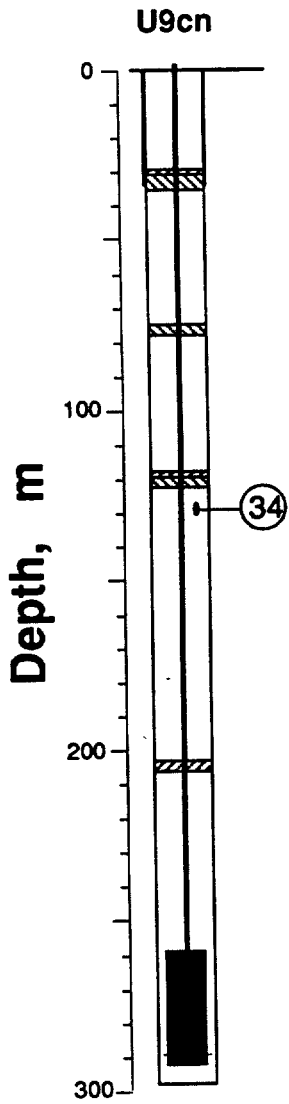


Figure 2.4 Pressure and radiation measured in the coarse stemming below plug 2 (station 34 at a depth of 128.0 m).

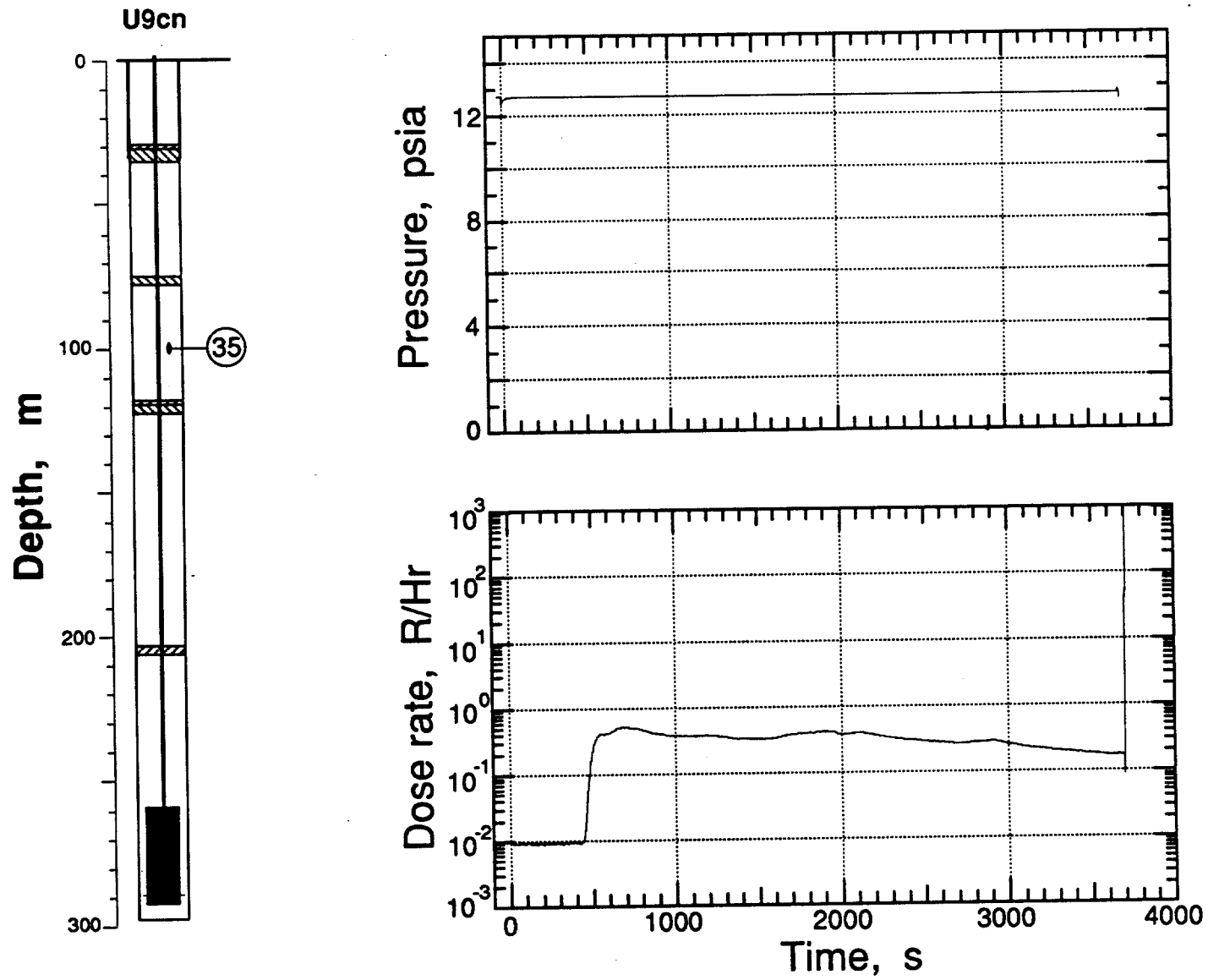


Figure 2.5 Pressure and radiation measured in the coarse stemming between plugs 2 and 3 (station 35 at a depth of 99.1 m).

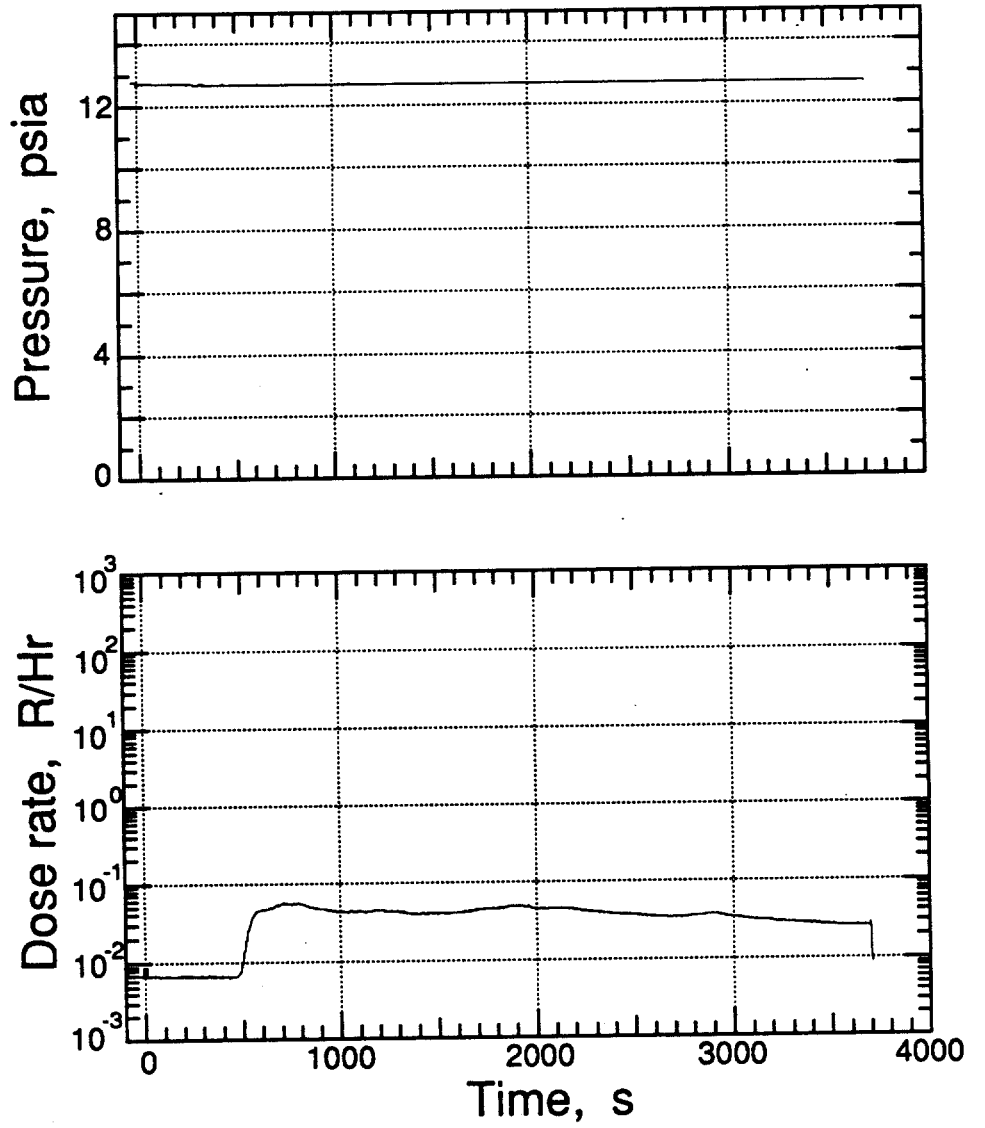
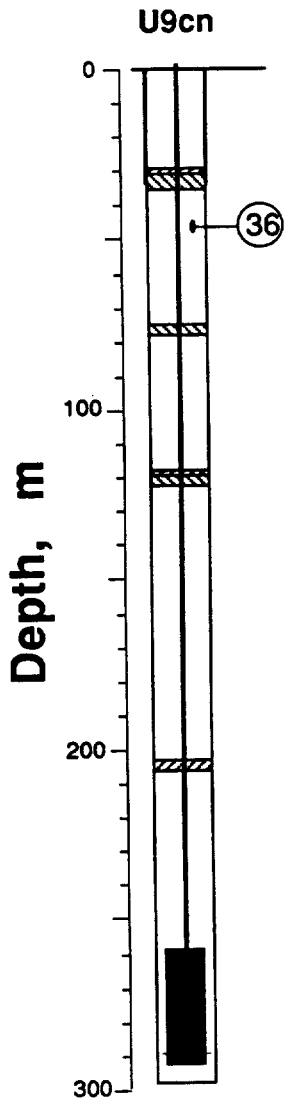


Figure 2.6 Pressure and radiation measured in the coarse stemming between plugs 3 and 4 (station 36 at a depth of 45.8 m).

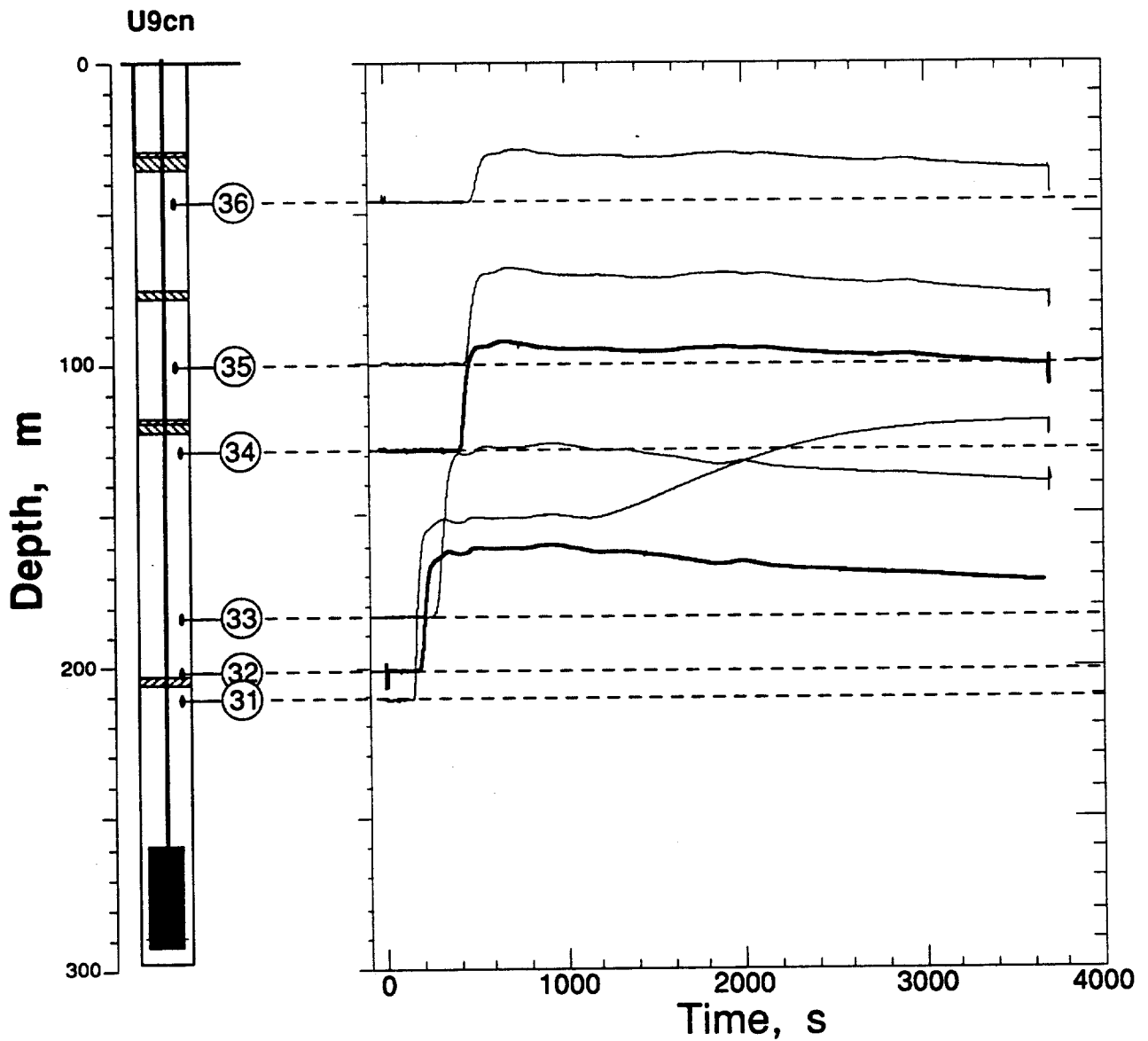


Figure 2.7 Composite plot of all of the radiation wave forms obtained on KESTI with the data from each station placed at its corresponding depth. All wave forms are to the same vertical scale (see figures 2.1 - 2.6 for absolute amplitudes) and the baseline of each is at 0.001 R/Hr. The data from stations 32 and 34 are accentuated for clarity.

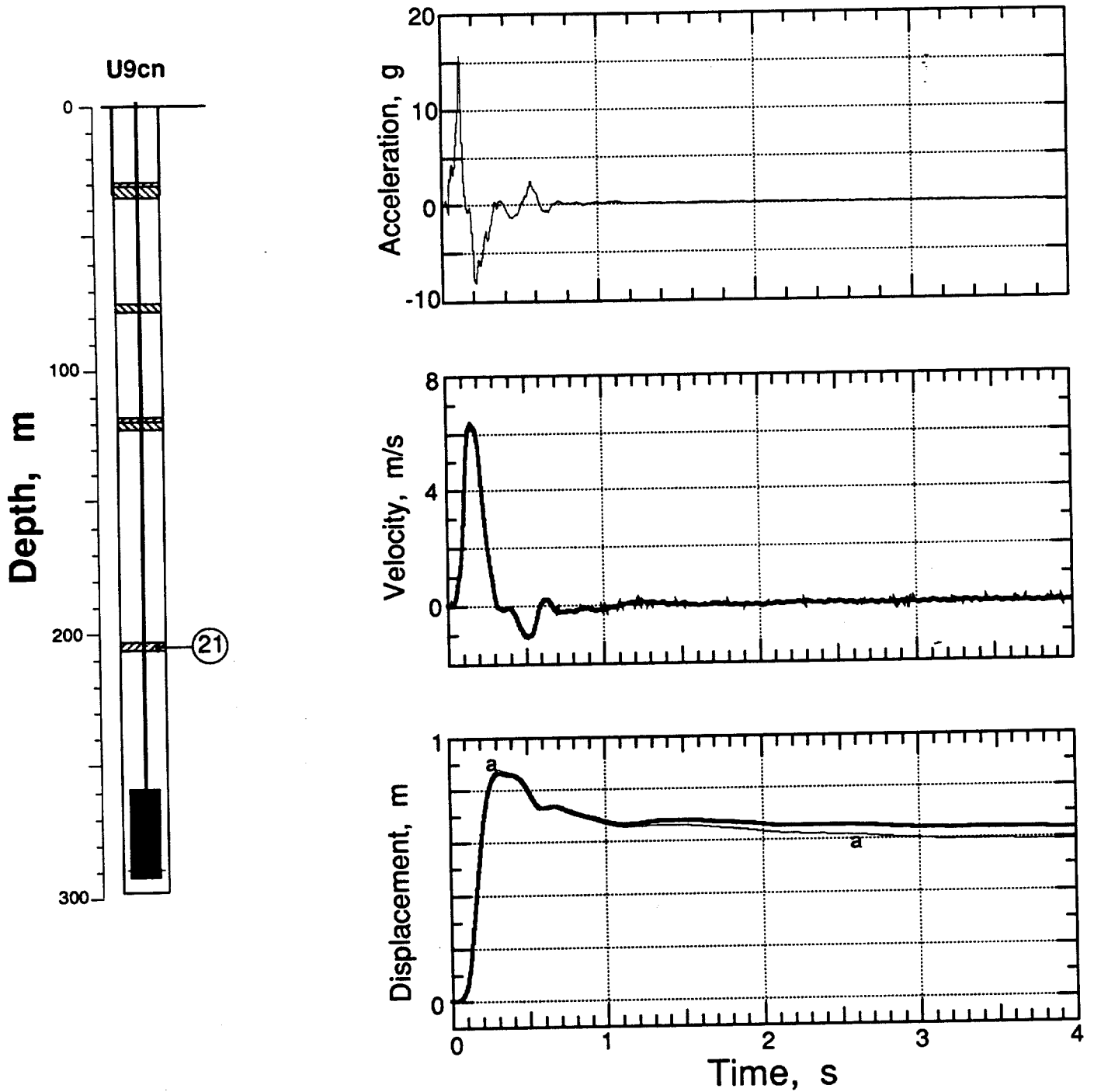


Figure 2.8 Explosion-induced vertical motion of the bottom plug (station 21 at a depth of 204.5 m) The traces annotated with "a" are derived from the acceleration while the velocimeter-derived signals are shown as heavy traces.

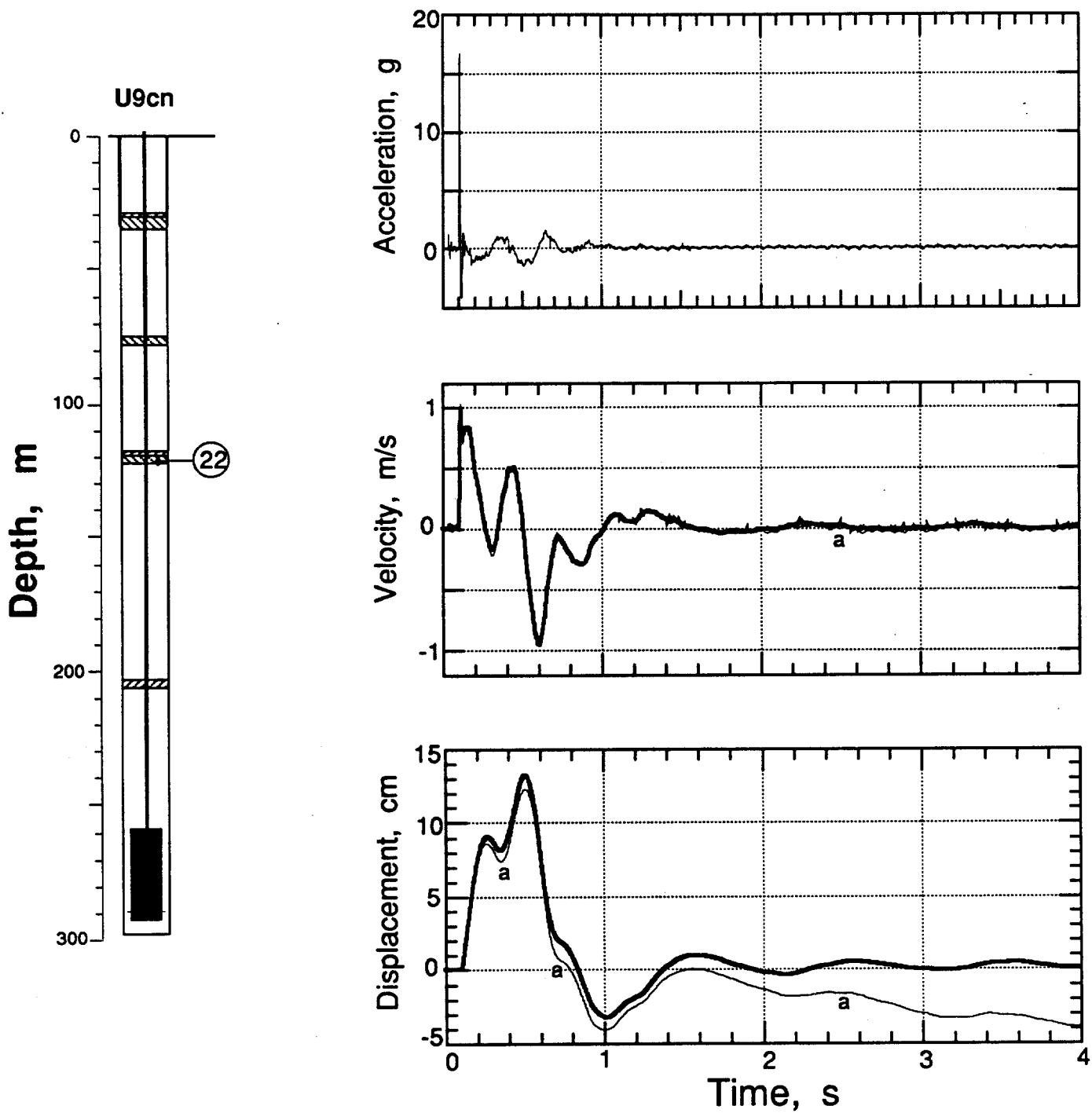


Figure 2.9 Explosion-induced vertical motion of plug 2 (station 22 at a depth of 120.4 m) The traces annotated with "a" are derived from the acceleration while the velocimeter-derived signals are shown as heavy traces.

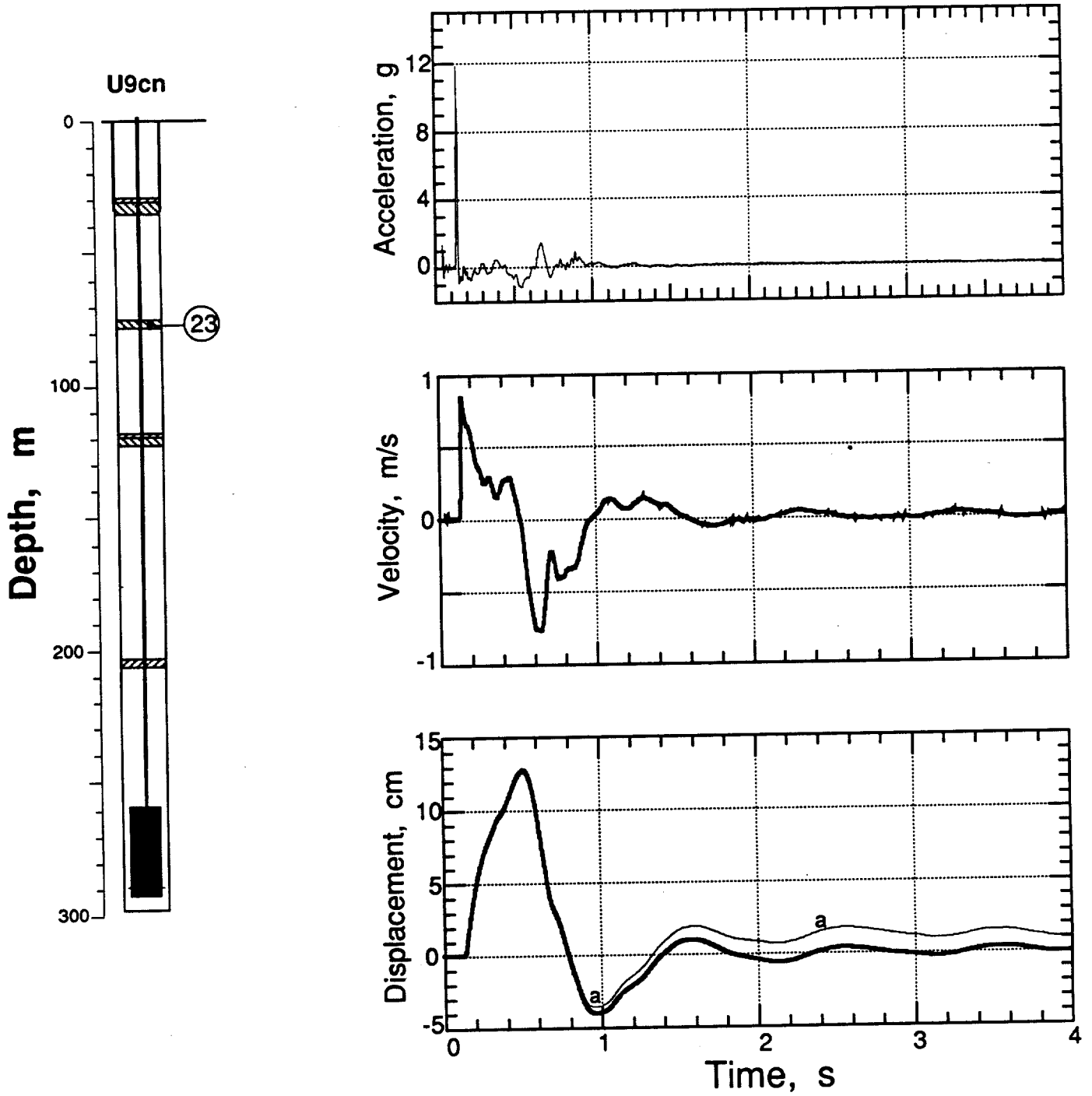


Figure 2.10 Explosion-induced vertical motion of plug 3 (station 23 at a depth of 76.5 m) The traces annotated with "a" are derived from the acceleration while the velocimeter-derived signals are shown as heavy traces.

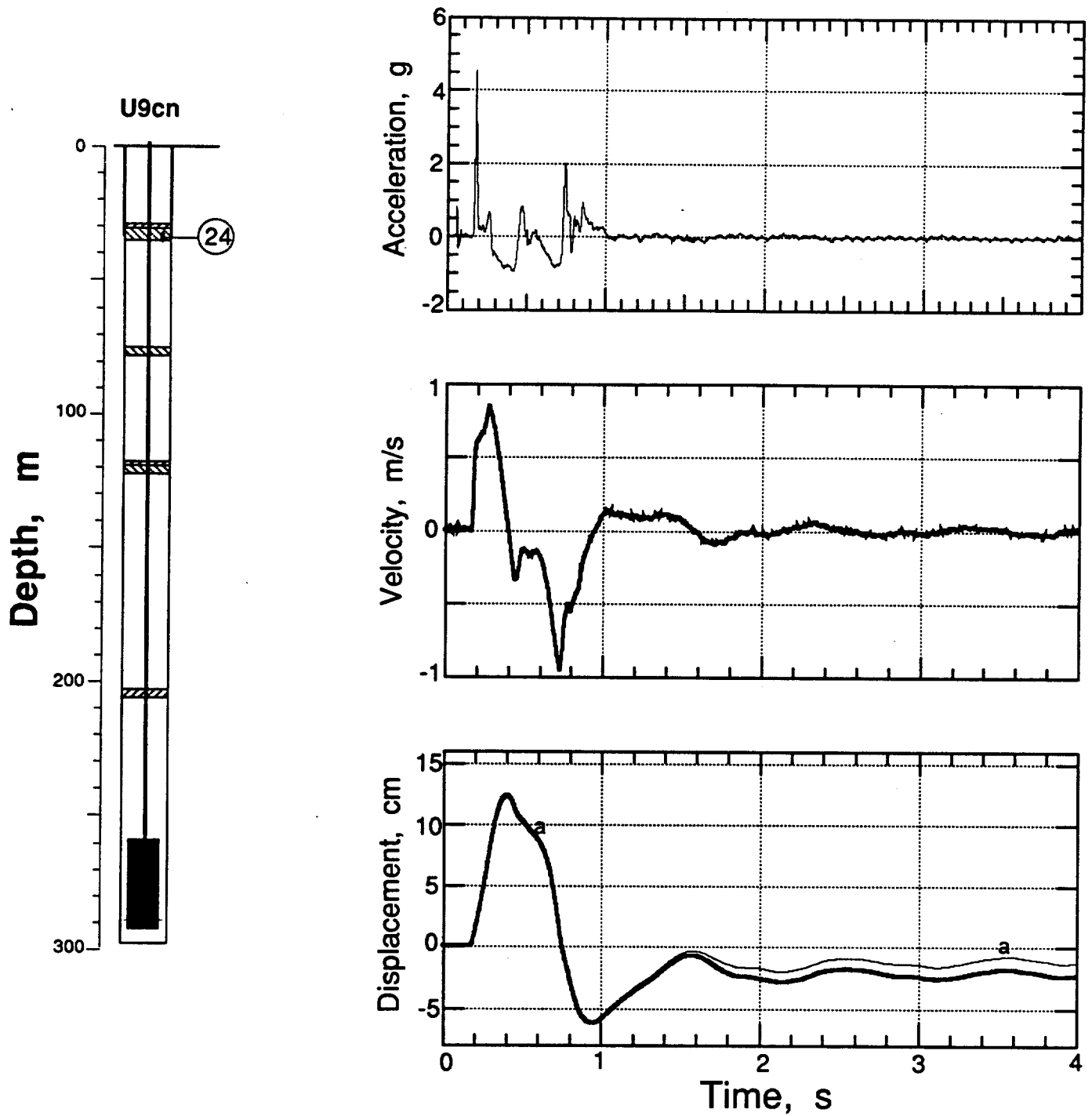


Figure 2.11 Explosion-induced vertical motion of the top plug (station 24 at a depth of 32.9 m) The traces annotated with "a" are derived from the acceleration while the velocimeter-derived signals are shown as heavy traces.

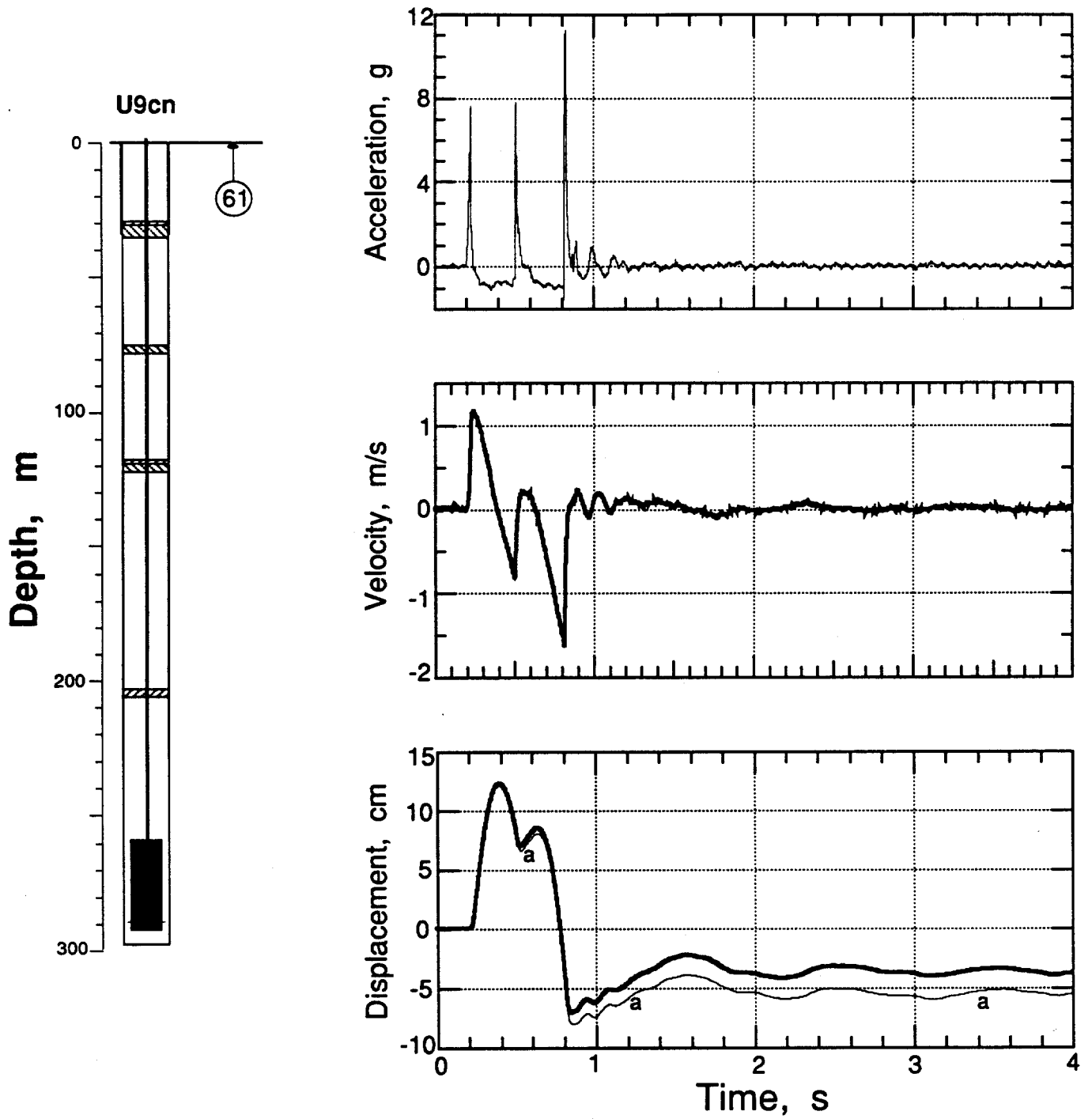


Figure 2.12 Explosion-induced vertical motion of the ground surface, 15.24 from SGZ (station 61 at a depth of 0.9 m) The traces annotated with "a" are derived from the acceleration while the velocimeter-derived signals are shown as heavy traces.

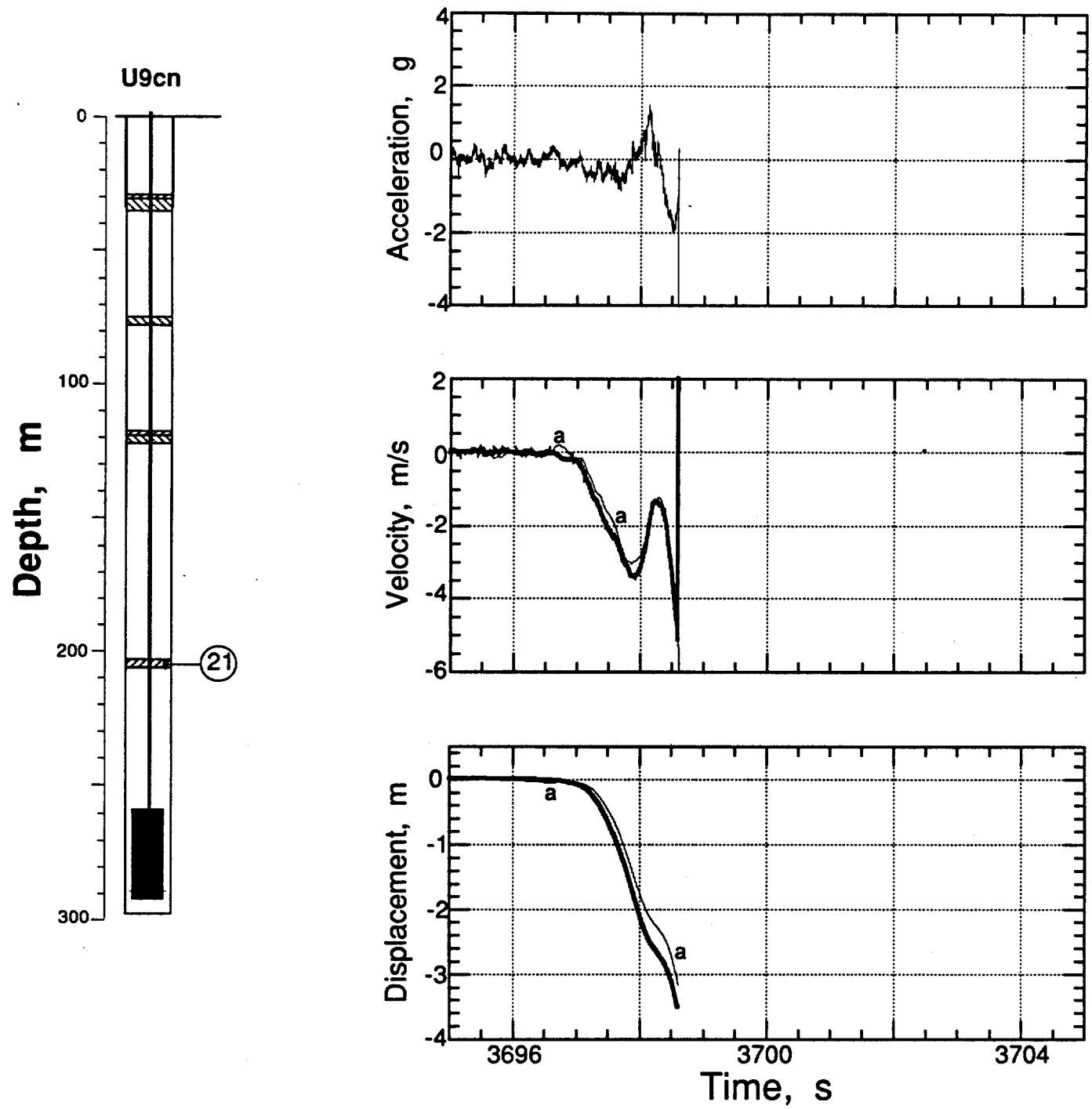


Figure 2.13 Collapse-induced vertical motion of the bottom plug (station 21 at a depth of 204.5 m) The traces annotated with "a" are derived from the acceleration while the velocimeter-derived signals are shown as heavy traces.

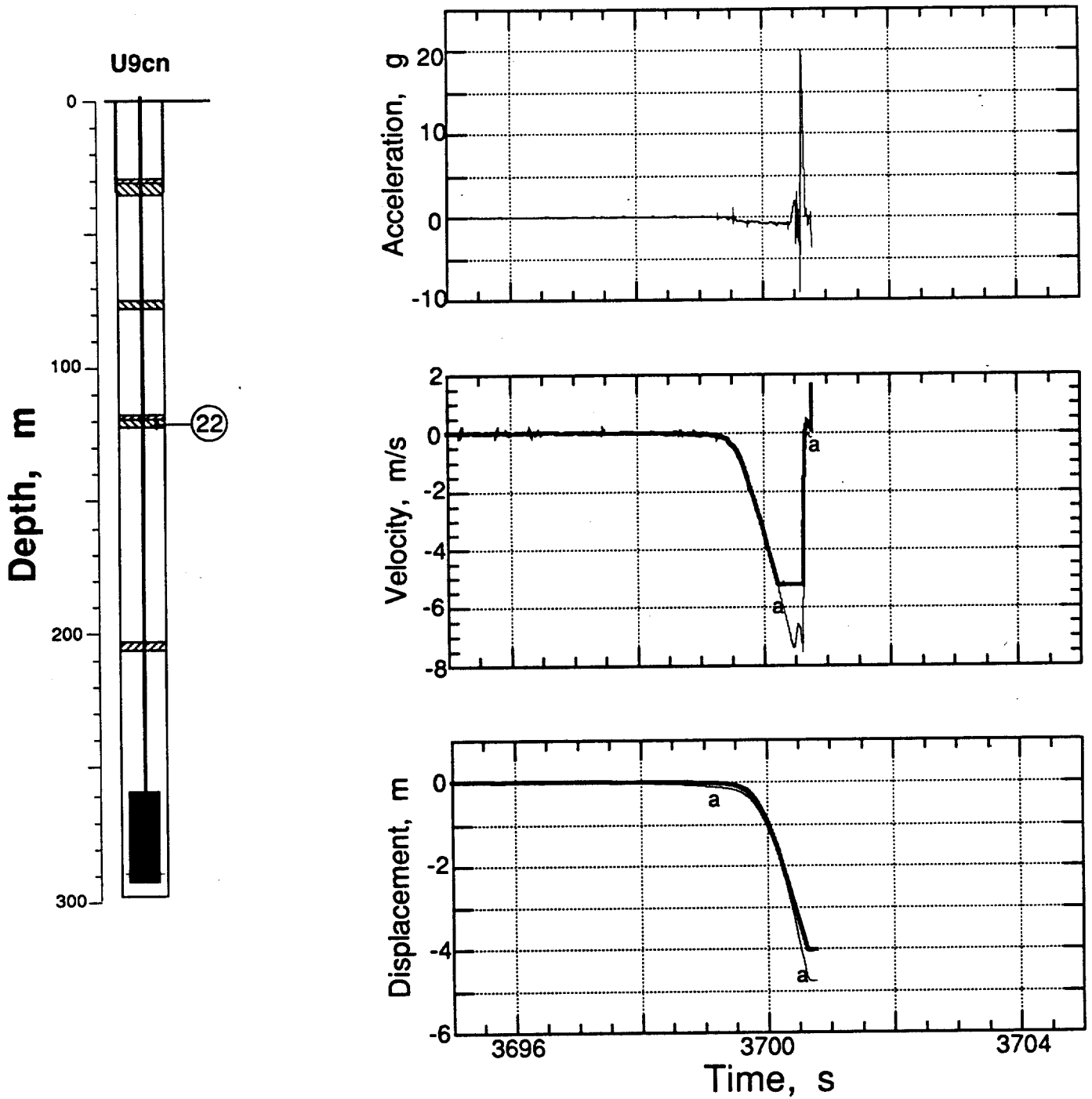


Figure 2.14 Collapse-induced vertical motion of plug 2 (station 22 at a depth of 120.4 m) The traces annotated with "a" are derived from the acceleration while the velocimeter-derived signals are shown as heavy traces.

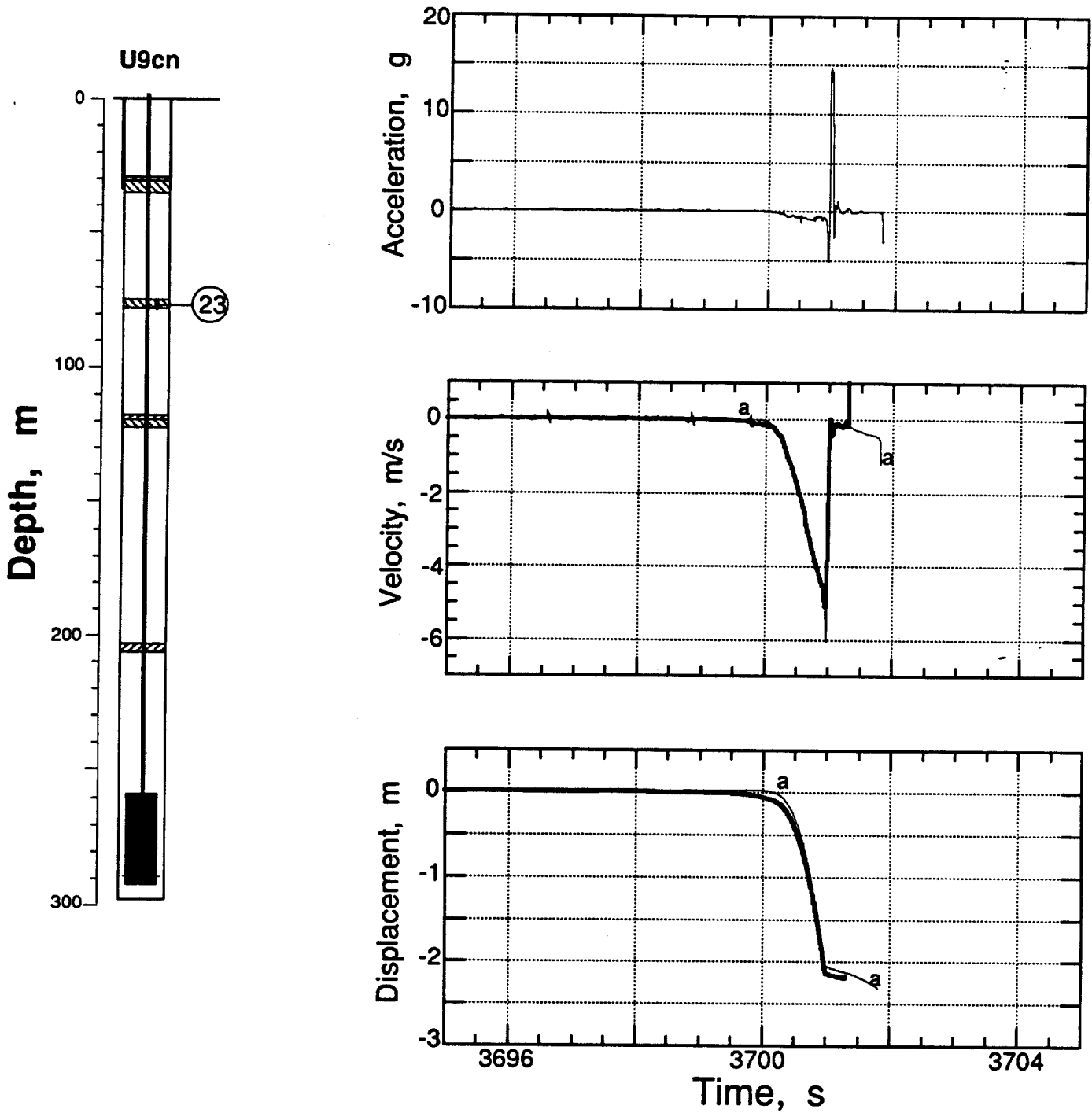


Figure 2.15 Collapse-induced vertical motion of plug 3 (station 23 at a depth of 76.5 m) The traces annotated with "a" are derived from the acceleration while the velocimeter-derived signals are shown as heavy traces.

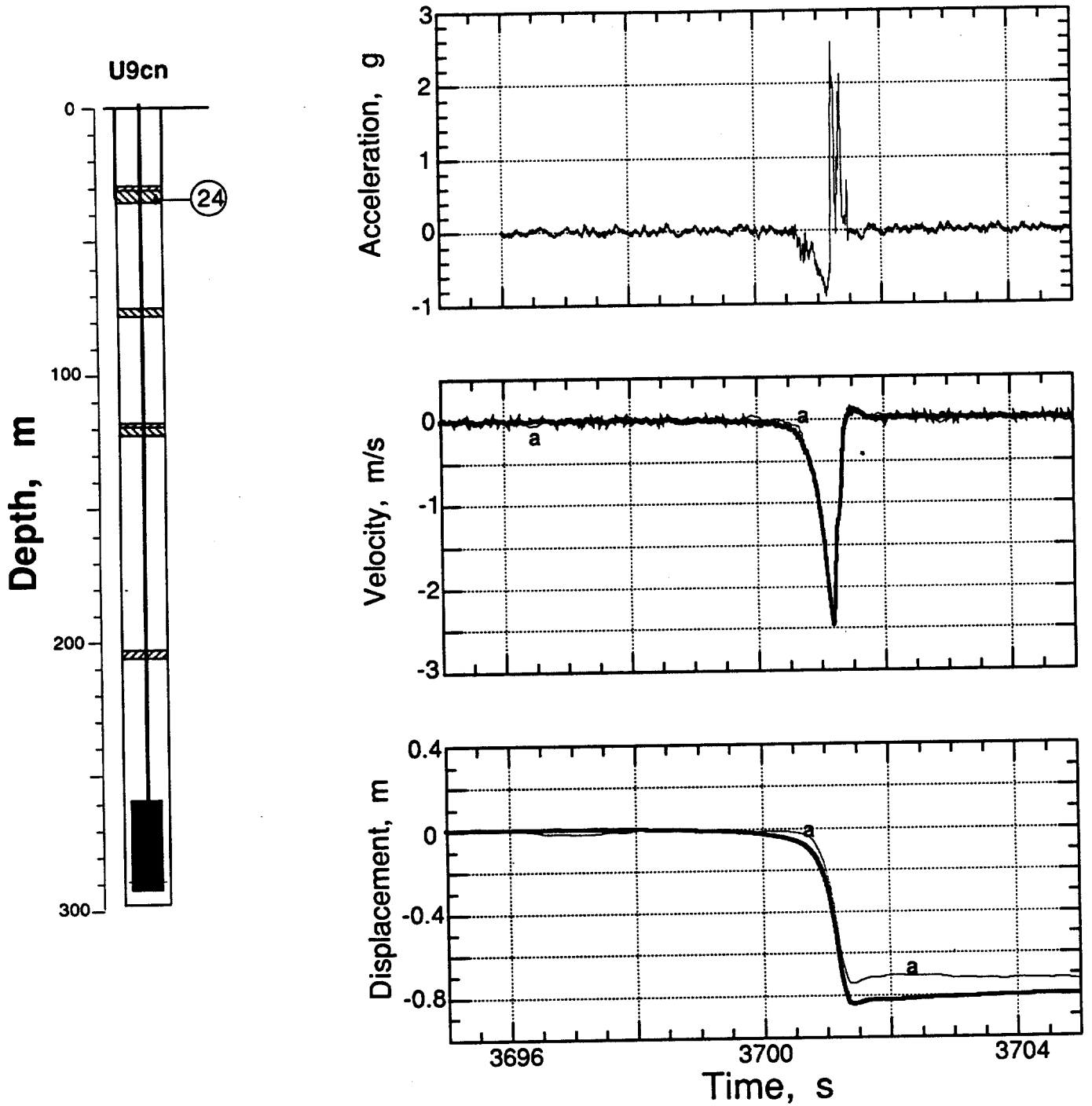


Figure 2.16 Collapse-induced vertical motion of the top plug (station 24 at a depth of 32.9 m)
 The traces annotated with "a" are derived from the acceleration while the
 velocimeter-derived signals are shown as heavy traces.

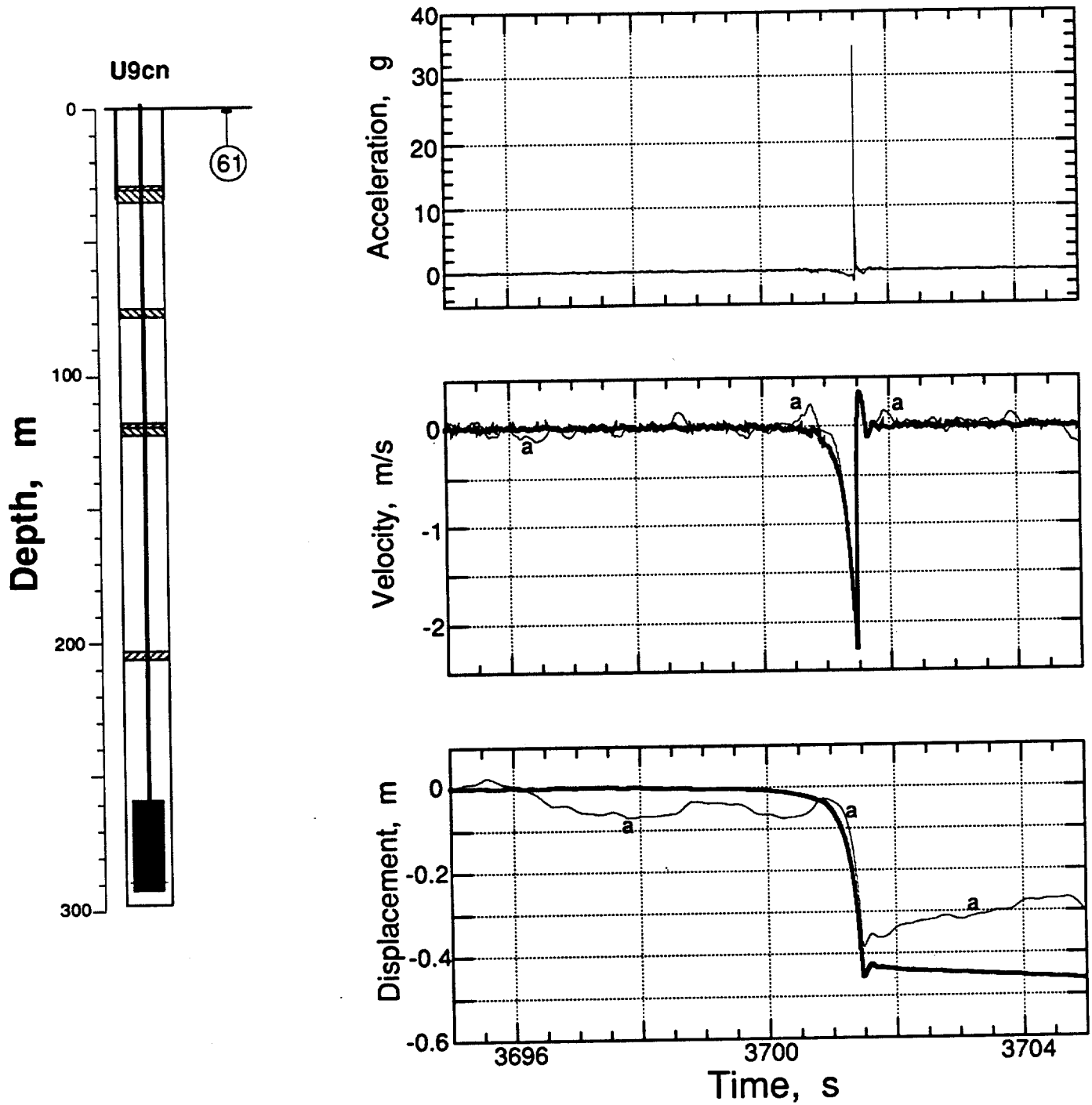


Figure 2.17 Collapse-induced vertical motion of the ground surface at a horizontal range of 15.24 m and a depth of 0.9 m (station 61). The traces annotated with "a" are derived from the acceleration while the velocimeter-derived signals are shown as heavy traces.

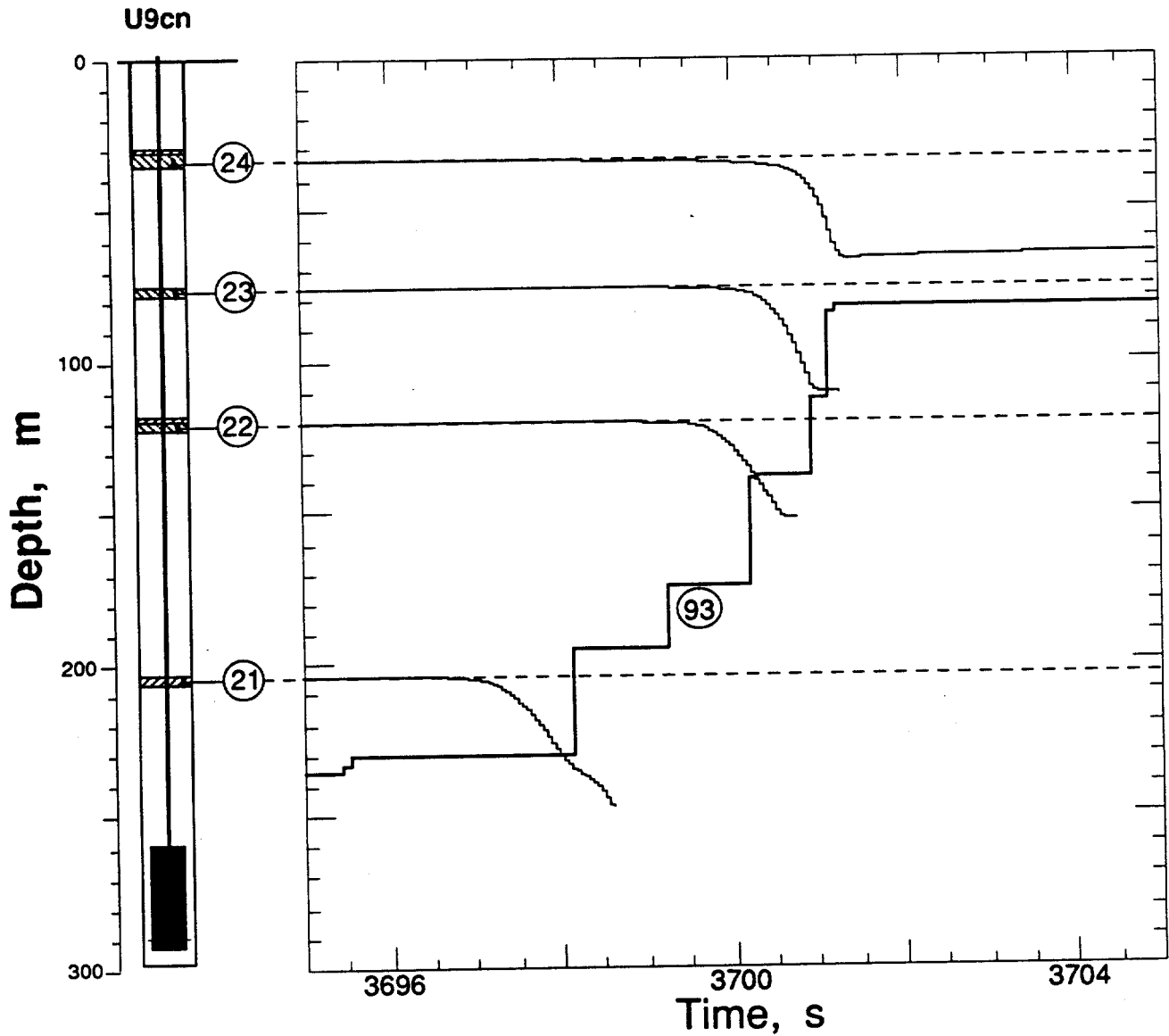


Figure 2.18 Progression of the collapse as indicated by the CLIPER record (station 93) and the displacement histories of the stemming plugs. The motion signal was lost at the termination of the respective trace. Displacement histories are NOT to the same vertical scale: they are shown for wave form only.

Table 2.1 Summary of Containment-Related Motion

Gauge	Slant Range (m)	Arrival Time (ms)	Acceleration Peak (g)	Velocity Peak (m/s)	Displacement Peak (cm)	Displacement Residual (cm)
21av	84.48	22.7(a)	15.7	6.4	87	59
21uv	84.48	22.7(a)	-	6.3	86	64
22av	168.6	38(a), 100	16.6	1.03	12.2	-4
22uv	168.8	38(a), 100	-	0.99	13.2	0
23av	212.5	48.5(a), 136.5	11.9	0.85	13.0	1.4
23uv	212.5	49(a), 136.5	-	0.85	12.6	0
24av	256.1	60(a), 165	5.1	0.83	12.1	-1
24uv	256.1	170	-	0.84	12.4	-2
61av	288.5	200	7.7, 11.3(b)	1.12	12.2	0
61uv	288.5	202	-	1.14	12.3	1.3

(a) Pipe-induced motion.

(b) Slap-down.

Table 2.2 Containment-Related Accelerometer Characteristics

<u>Gauge</u>	<u>Natural Frequency (Hz)</u>	<u>Damping Ratio</u>	<u>System Range (g's)</u>
21av	810	0.65	80
22av	348	0.75	16
23av	360	0.65	12
24av	326	0.75	20
61av	620	0.65	40

Table 2.3 Containment-Related Velocimeter Characteristics

<u>Gauge</u>	<u>Natural Frequency (Hz)</u>	<u>Time to 0.5 Amplitude (s)</u>	<u>Calibration Temperature (°F)</u>	<u>Operate Temperature (°F)</u>	<u>System Range (m/s)</u>
21uv	3.56	9.52	74.6	84.7	16
22uv	3.80	8.2	73.5	91.3	4
23uv	3.50	11.25	74.9	93.0	4
24uv	3.50	9.32	73.7	94.7	6
61uv	3.56	9.75	74.5	68.21	10

3. Other measurements

Pressure and temperature were monitored in a line-of-sight pipe within the diagnostics canister at locations on either side of a baffle in the line-of-sight. Wave forms of these quantities are shown, for completeness, in figures 3.1 and 3.2. Signals from these transducers were corrupted after 40 ms and the data are otherwise questionable.

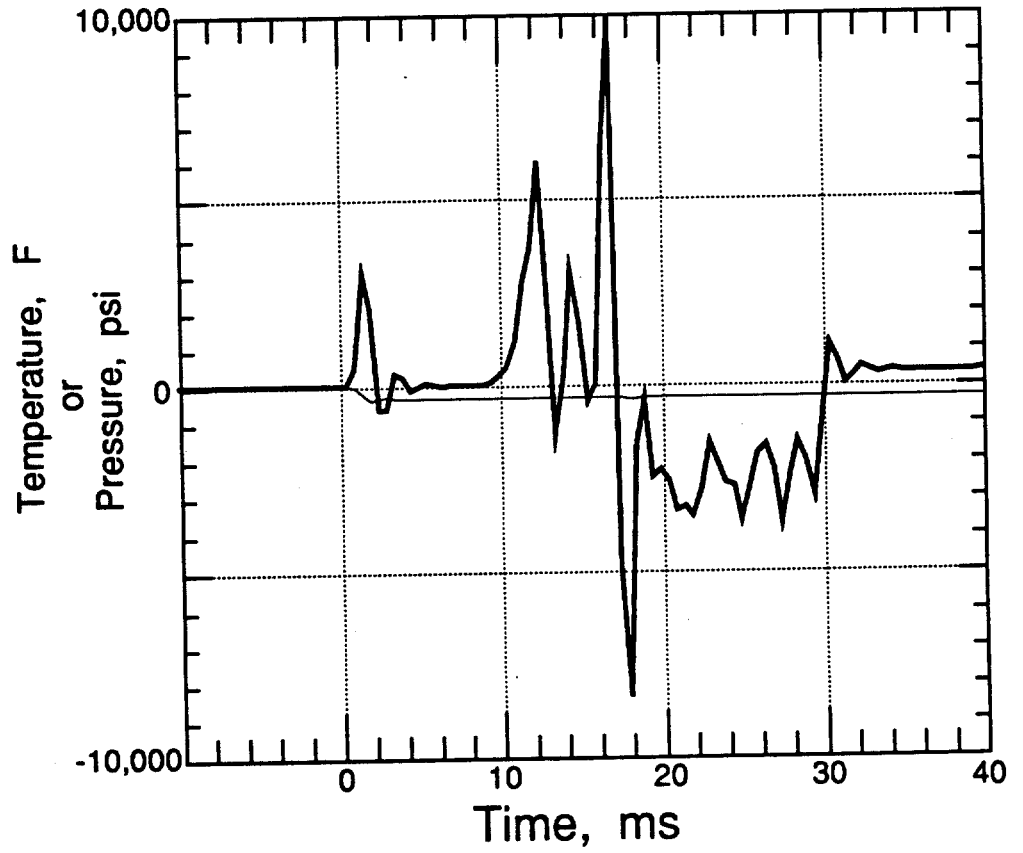
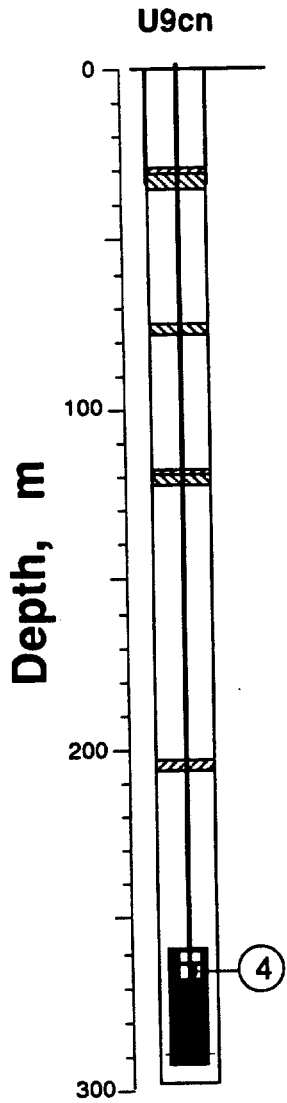


Figure 3.1 Pressure and temperature measured in a line-of-sight pipe on the device side of a baffle (station 4 at a range of 24.1 m from the device). The heavier trace represents pressure.

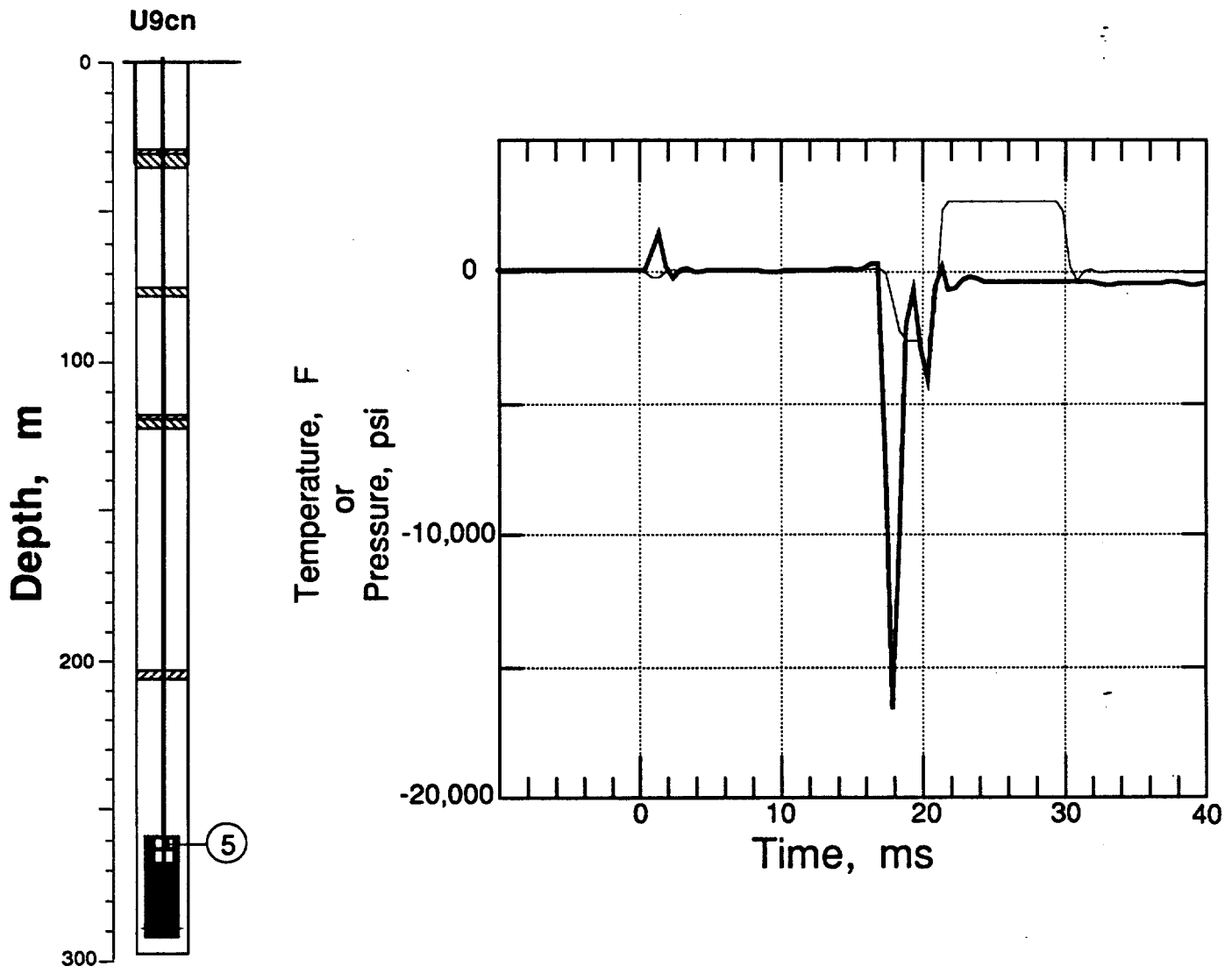


Figure 3.2 Pressure and temperature measured in a line-of-sight pipe on the up-stream side of a baffle (station 5 at a range of 27.1 m from the device). The heavier trace represents pressure.

References

1. N. W. Howard, "U9cn Preliminary Site Characteristics Summary", DM 81-84, Lawrence Livermore National Laboratory, Livermore, CA, December 21, 1981.
2. George Kronsbein, "Containment Report for U9cn," Holmes & Narver, NTS:A2:82-59, June 9, 1982.
3. LLNL contacts for additional information: R. A. Heinle (CORTEX and SLIFER data)
4. William G. Webb, "Special Measurements Final Engineering Report on KESTI, U9cn", EG&G, Energy Measurements, Las Vegas, NV, SM:82E-95-35, 26 July, 1982.
5. William G. Webb, "Special Measurements Physics/Instrumentation Package for KESTI, U9cn, , Revision 'A' ", EG&G, Energy Measurements, Las Vegas, NV, SM:82E-95-34, 23 July, 1982.
6. E. C. Woodward "KESTI Containment Diagnostics Report", UOPKL 82-98, Lawrence Livermore National Laboratory, Livermore, CA, November 29, 1982.

Distribution:

LLNL

TID (11)	L-053
Test Program Library	L-045
Containment Vault	L-221
Burkhard, N.	L-221
Cooper, W.	L-049
Denny, M.	L-205
Goldwire, H.	L-221
Hannon, W. J.	L-205
Heinle, R. (5)	L-221
Mara, G.	L-049
Moran, M. T.	L-777
Moss, W.	L-200
Patton, H.	L-205
Pawloski, G.	L-221
Rambo, J.	L-200
Roland, K.	L-221
Roth, B.	L-049
Valk, T.	L-154

LANL

App, F.	F-659
Brunish, W.	F-659
Kunkle, T.	F-665
Trent, B.	F-664

Sandia

Bergstresser, T.	MS-1159
------------------	---------

BNL/AVO

Brown, T.	A-5
Hatch, M.	A-5
Still, G.	A-5
Stubbs, T.	A-5

BNL/NVO

Bellow, B.	N 13-20
Davies, L.	N 13-20
Moeller, A.	N 13-20
Robinson, R.	N 13-20
Webb, W.	N 13-20

DNA

Ristvet, B.

S-Cubed

Peterson, E.

Eastman Cherrington Environment
1640 Old Pecos Trail, Suite H
Santa Fe, NM 87504

Keller, C.

Technical Information Department • Lawrence Livermore National Laboratory
University of California • Livermore, California 94551

